Modeling And Testing Of R23/R134a Mixed Refrigerant System With Water Cooled Separator For Low Temperature Refrigeration

Nicholas Hugh
Marquette University

MODELING AND TESTING OF R23/R134A MIXED REFRIGERANT SYSTEM WITH WATER COOLED SEPARATOR FOR LOW TEMPERATURE REFRIGERATION

By

Nicholas Hugh

A Thesis submitted to the Faculty of the Graduate School,
Marquette University,
in Partial Fulfillment of the Requirements for
the Degree of Master of Science

Milwaukee, Wisconsin

May 2013

ABSTRACT
MODELING AND TESTING OF R23/R134A MIXED REFRIGERANT SYSTEM WITH WATER COOLED SEPARATOR FOR LOW TEMPERATURE REFRIGERATION

Nicholas Hugh

Marquette University, 2013

Low temperature (LT, -35 °C to -50 °C) and ultra low temperature (ULT, -50 °C to -100 °C) refrigeration is required in the life sciences industry for the production and storage of biological systems. The minimum practical storage temperature of a simple, single-stage refrigeration system is -30 °C, and this is incapable of meeting the requirements of biotechnology applications. Current LT and ULT refrigeration systems utilize cascade systems, which are combinations of single-stage refrigeration systems operating at successively lower temperatures. Because they use multiple compressors, cascade systems have higher capital and operating costs than simple single-stage vapor compression refrigeration systems. Equipment operating costs of LT and ULT refrigeration contribute significantly to the operating costs of biotechnology companies and therefore motivate the development of lower cost, higher performance refrigeration systems.

One approach to achieving greater efficiency is the development of single compressor systems that utilize a refrigerant mixture and a condensing separator. After compression, the refrigerants are separated and follow refrigeration cycles similar in working temperature and pressure to cascade systems to achieve the desired temperature and heat load capacity. The refrigerant mixture streams are combined at the suction side of the compressor and compressed again to complete the cycle. This concept has the benefit of using a single compressor to reach low temperatures rather than the multiple compressors used in cascade systems.

This work addresses the modeling, analysis and testing of a single compressor mixed refrigerant system (MRS) for low temperature applications. A model will be developed using first and second law principles of thermodynamics to calculate the refrigeration capacity, power consumption, coefficient of performance (COP), and second law efficiency. The model results will be validated through comparison with experimental results for a prototype system under steady-state conditions. Also, the model results will be explored to determine the impact of mixture composition on the system performance. Performance and benefits of the MRS will be compared to a similar cascade refrigeration system operating under similar conditions. The experimental performance of the prototype MRS will be used to make recommendations to advance the development of more efficient low temperature storage refrigeration systems.

ACKNOWLEDGEMENTS

Nicholas Hugh

I would like to thank Dr. Anthony Bowman and Dr. Margaret Mathison for their guidance and support as my thesis advisors. Also, the Marquette University Department of Mechanical Engineering for the support and facilities to accomplish my thesis objectives. I would like to thank Scott Farrar for being a member of my thesis committee.

I am grateful for the support of Scott Farrar and the members of Farrar Scientific for their materials, guidance and expertise throughout the development of the thesis project.

I would like to thank Mark Hugh of Selarity Refrigeration for his assistance and guidance while fulfilling my thesis requirements at Marquette University.

Thank you to Annette Wolak for her assistance throughout my graduate studies at Marquette University.

Finally, a special thanks to my parents, Mark and Sandy, for their love and support. You have given me the tools, not only to achieve great educational milestones, but to continue to fulfill my dreams.

TABLE OF CONTENTS

LIST OF TABLES

LIST OF FIGURES

Chapter 1

Introduction

Low temperature refrigeration for the life sciences industry is concerned with the use of refrigeration cycles to provide cooling to freeze products for thermal storage. Freezing biological products at low temperatures retards the degradation of microbiological tissue, therefore, enhancing the shelf life of the product. Increasingly lower storage temperatures correlate with lengthening preservation effects. The American Society for Heating, Refrigeration and Air Conditioning (ASHRAE) defines low temperature (LT) refrigeration in the range of -30 °C to -50 °C (-22 °F to -58 °F), and ultra-low temperature (ULT) refrigeration from -50 °C to -100 °C (-58 °F to -148 °F). ULT refrigeration for long term storage is the focus of the research presented in this thesis. Refrigeration systems used for long term sample storage consume large amounts of electricity because they operate continuously. Power consumption is the leading contributor to operational costs of low temperature refrigeration systems.

Development of novel refrigeration systems that reach low temperatures while improving performance will provide a more energy efficient product for the biotechnology industry. This chapter reviews the present state of LT and ULT refrigeration and defines the design parameters that will be used for the modeling and testing of a mixed refrigerant low temperature system.

1.1 Ultra Low Temperature Refrigeration Applications

Functions for low temperature refrigeration involve applications to various industries such as low temperature storage, chemical processing, manufacturing and biological preservation. These categories can be divided into two processes, freezing and refrigeration.

The process of freezing employs a refrigeration system to freeze a substance at a particular temperature where it can be stored in order to preserve its shelf life. This is done using

oversized refrigeration systems to freeze the substance under specified time constraints. It has been shown that freezing a substance more quickly will increase the shelf life of the substance by slowing the degradation affects of biological entities (Wallace, 1964). Refrigeration systems that are used for freezing substances consume high amounts of electricity but do not operate continuously. These systems are used only during the freezing process, and then the substances are relocated to a system that will hold them at constant temperature for long periods of time.

Once substances are frozen they are transported to refrigeration systems built to maintain low temperatures for long term storage. Since the samples that are placed in long term storage systems are already at the specified temperature, the system must remove significantly less energy to maintain the temperature. This allows the refrigeration system to maintain low temperatures while removing a smaller heat load which leads to the use of compressors with lower refrigeration capacities. The process of freezing and storing samples is more efficient with separate systems because compressors consume the majority of the power in refrigeration cycles. Dividing the freezing and refrigeration storage processes into two separate systems provides an efficient process for samples to reach low temperatures, but refrigeration storage systems are continuously operated leading to high operational costs. Research of storage refrigeration systems to increase the performance and lower operational costs will provide more efficient products for biotechnology companies.

1.2 Temperature and Heat Load Requirements

Low temperature and ultra low temperature refrigeration storage systems operate at various temperatures depending on the substance being stored. The current analysis focuses on applications with an evaporator temperature of -80 °C (-112 °F) because it is a common set point for laboratory refrigeration systems used for long term sample storage (Panasonic, 2012 and Thermo Fisher Scientific, 2007). To maintain a sample temperature of -80 °C (-112 °F), the typical systems supply refrigerant to the low stage evaporator at a maximum temperature of -85

°C (-121 °F). This ensures that the refrigerant absorbs sufficient heat to keep a nearly constant compartment temperature of -80 °C (-112 °F). Single-stage refrigeration systems are commonly used to reach temperatures near -30 °C (-22 °F), but more complex cascading refrigeration cycles are currently used for ULT applications near -80 °C (-112 °F). Although cascade refrigeration is an effective way to reach low evaporating temperatures, the systems do not achieve high coefficients of performance (COP) while removing the required heat loads at -80 °C (-112 °F).

Relatively small heat loads compared to air conditioning and food storage refrigeration, on the order of hundreds of Watts versus thousands of Watts, are required to maintain an evaporation temperature of -80 °C (-112 °F). The engineers at Farrar Scientific and Selarity Refrigeration have worked with ULT refrigeration throughout the past 25 years and have developed a standard heat load for common cabinet sizes ranging from 0.37 to 0.76 m^3 (13 to 27 ft^3). Their experience has indicated that a head load of 161.2 W (550 Btu/hr) must be removed from the cabinet to maintain a temperature of -87 °C (-124.6 °F). An additional 25% of 161.2 W (550 Btu/hr) , suggested by the engineers at Farrar Scientific and Selarity Refrigeration, is added to the heat load to determine the total heat load that must be removed from the cabinet, 256.4 W (875 Btu/hr). For this work, a total heat load of 256.4 W (875 Btu/hr) is used with a 25% safety factor to provide a conservative evaporator heat load for the system analysis. ULT storage devices are designed for constant heat loads because the cabinet is assumed to be full at all times, are not opened frequently to access samples, and must be maintained at the specified evaporator temperature.

1.3 Current ULT Equipment

The majority of current ULT refrigeration designs are cascade systems that use two refrigeration cycles in series to reach low evaporating temperatures. Current ULT refrigeration centers on cascade cycles due to their well known design characteristics and use of refrigerant blends that have low environmental impacts. Although ULT cascade systems are an effective

way to reach low temperatures, their two compressors consume more power leading to sub-optimal coefficients of performance. Research to advance ULT refrigeration is focused on two main areas: cascade cycle improvement and alternative refrigeration cycle design.

Cascade cycle improvement is closely linked to the enhancement of individual components and it focuses on the optimization of currently used system configurations. Compressors are the main component of a refrigeration cycle; as such, there are numerous studies working to continually enhance efficiency. Refrigeration cycles also consist of a condenser, where heat is rejected to a medium, and an evaporator, where heat is absorbed by the refrigerant. Heat exchangers are a common cause of cycle inefficiency and are also an important focus of current research (Mehrabian & Samadi, 2010). With the improvement of software algorithms, numerical techniques have been a focus of research to optimize current refrigeration cycle equipment (Parekh, Tailor & Jivanramajiwala, 2010).

Advancement of new refrigerant blends has led to the development of alternative refrigeration cycles for ULT systems. Current equipment is used in various configurations in order to research their impact on overall cycle performance; several configurations will be described in more detail in section 2.3. Multiple compressors can be eliminated in new design configurations, which allow for significant reduction in the power required to operate a system. Research is designed to improve the coefficient of performance for refrigeration cycles, and to provide new alternatives to reach lower and lower temperatures in the ULT refrigeration range.

Chapter 2

Background

A refrigeration process is performed when a heat load is removed from a specified space in order to reduce the temperature below the atmospheric temperature. The space could be the inside of a home where air conditioners are used or it could be a refrigerator where products are stored at a specified temperature. The modern vapor-compression refrigeration cycle consists of a condenser and an evaporator where heat is rejected from the working fluid to a sink and heat is absorbed by the working fluid from the storage space, respectively. The cycle is driven by a compressor, where the working fluid is compressed in vapor form from a low pressure and low temperature to a high pressure and high temperature. Numerous processes are used to complete the cycle from the condenser to the evaporator and vary from simple single-stage cycles to mixed refrigerant systems. Common refrigeration system designs for low temperature refrigeration that lead to the design of mixed refrigerant cycles will be discussed in order of increasing complexity and decreasing evaporation temperature range.

2.1 Single-Stage Refrigeration Systems

A simple vapor-compression system is presented in Figure 2.1 and uses one compressor for its operation; single-stage refers to a single compressor. A single-stage vapor-compression system consists of a compressor, condenser, expansion device and an evaporator. The cycle begins as a working fluid is compressed in the vapor state (state 1) from low pressure to a high pressure and temperature, and flows into a condenser (state 2). In the condenser, heat is removed from the fluid, by rejection to the environment, and it is condensed to a saturated liquid state. After the condenser (state 3) the fluid flows into an expansion device where it expands from high pressure and high temperature to low pressure and low temperature at nearly constant enthalpy.

At this point the fluid is in a mixed liquid-vapor phase and flows into the evaporator (state 4). As the fluid flows through the evaporator it absorbs heat from the refrigerated space and evaporates, leaving the evaporator as a saturated vapor, or slightly superheated vapor entering the compressor to complete the cycle (state 1).

The cooling effect happens in the evaporator as the working fluid is absorbing energy from the refrigerated space. Exiting the expansion device, the working fluid is at a low temperature, and this is the lowest temperature the working fluid will reach, but the refrigerated space cannot be controlled at this temperature. For heat transfer to occur the refrigerated space must be controlled at a temperature at least 2.8 °C (5 °F) above that of the working fluid entering the evaporator. This practical minimum temperature difference will allow for enough heat to be transferred from the refrigerated space to the working fluid so that it will leave as a saturated vapor or slightly superheated vapor state. Otherwise, if the working fluid leaves the evaporator as a liquid-vapor mixture, damage will be caused to the compressor because it is not totally in a compressible state.

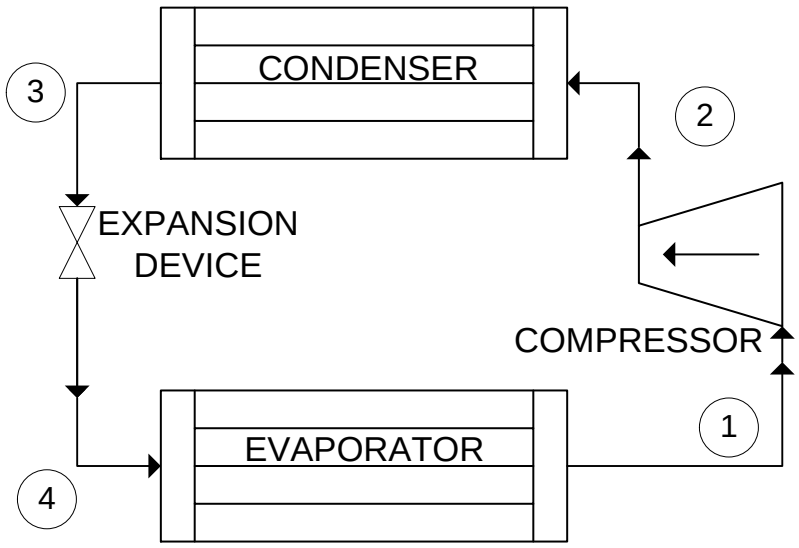

Figure 2.1: Single-stage, vapor-compression refrigeration system.

Single-stage refrigeration systems are used for many applications, but generally are limited to evaporating temperatures above 0 °C (32 °F) with some temperature applications reaching near -30 °C (-22 °F) . Several industries are concerned with refrigeration temperatures near -30 °C (-22 °F), but many life science and chemical production practices require temperatures much lower. Properties of the working fluids as well as the physical components limit the performance of single-stage systems at low temperatures, but primarily the system performance and capability are dictated by the performance of the compressor.

The most widely spread use of single-stage refrigeration systems, that reach temperatures near -50 °C (-58 °F), are blast freezers that use a compound or multi-stage compressor. A compound compressor is one which has two separate compression processes in series to reach very high compression ratios between the suction and discharge lines in the system. Although the compressor has multiple stages, the cycle is considered single-stage because the expansion process occurs in a single stage. Blast freezers are single-stage refrigeration cycles that can remove a large heat load in a short period of time while freezing products down to temperature of -30 °C to -50 °C (-22 °F to -58 °F). Systems that use compound compressors are expensive and consume large amounts of energy so they are generally only used for freezing and not refrigeration storage. Limitations on the performance of the single-stage refrigeration cycles led to the development of cascade refrigeration to reach ultra-low temperatures.

2.2 Cascade Refrigeration Systems

For ULT refrigeration to reach temperatures from -50 °C to -100 °C (-58 °F to -148 °F), an extremely large pressure difference across the expansion device is required. Present compressors cannot achieve sufficiently high compression ratios without malfunctioning. Therefore, a cascade refrigeration system was developed to achieve low temperatures using multiple compressors to cover such a great pressure difference. Cascade refrigeration systems consist of multiple single-stage vapor-compression refrigeration cycles in series.

Each successive single-stage refrigeration cycle in a cascade system drops the evaporating temperature toward the desired operating temperature. The single-stage cycles are linked through an inter-stage heat exchanger that acts as the evaporator for high-stage cycle and the condenser for the low-stage cycle; the refrigeration cycles are independent of one another and the refrigerants of one cycle do not mix with the one from another cycle. The high-stage and low-stage cycles may use the same refrigerants, but frequently the low-stage cycle's refrigerant is chosen for its optimal thermo-physical properties at the lower operating conditions. Although cascade refrigeration systems may consist of numerous single-stage cycles, two single-stage cycles are sufficient to reach temperatures in the ULT range,-50 °C to -100 °C (-58 °F to -148 °F). Two-stage cascade systems use the same or similar compressors that operate at a significantly lower compression ratios than one compressor would need in order to reach low temperatures. Cascade systems are more efficient, but consume more overall power than conventional single-stage refrigeration systems for such low evaporating temperatures. Low temperature refrigeration reached by a cascade system is conventionally used for storage and operate continuously. Improving the cycle efficiency of ULT cascade refrigeration systems will lower the operational cost for consumers and abate their overall impact on the environment.

2.3 Evolution of Mixed Refrigerant Systems

As the evolution of design improvements to single-stage and cascade systems produce cycles capable of achieving very low temperatures, testing was performed on common refrigerants and determined they are harmful to the environment. A need for refrigerant compounds that are less detrimental to the environment and still have advantageous thermodynamic properties at low temperatures brought about refrigerant blends formed from existing refrigerant compounds. As studied by Missimer (1997), new refrigerant blends brought improved cascade refrigeration cycle performance while replacing harmful chlorofluorocarbons with non-toxic and less environmentally detrimental chemicals. Theoretical analyses of

alternative refrigerant mixtures for single stage vapor-compression refrigeration cycles by Dalkilic and Wongwises (2010) have found new mixtures with enhanced thermodynamic properties.

Various refrigerant mixtures were experimentally studied by Gong et al. (2009) in a two-stage cascade refrigeration cycle to analyze coefficient of performance (COP), cooling capacity, pressure ratio, and discharge temperatures. Binary refrigerant mixtures of R170/R23, R170/R116 and a ternary mixture of R170/R23/R116 were used as the low stage refrigerant to compare overall performance values to those of R508B (the standard low temperature refrigerant used to reach -80 °C (-112 °F)). Results showed that the refrigerant mixtures operated at lower compression ratios with similar overall COP values and provided higher cooling capacities compared to R508B.

The potential performance enhancements of refrigerant mixtures in cascade cycles influenced designs for single-stage refrigeration systems. An experimental study of room temperature refrigeration by S.G. Kim and M.S. Kim (2002) achieved increased cooling capacity with binary mixtures of R744 (Carbon Dioxide)/R134a and R744/R290 for increasing mass fraction of R744. This was accomplished with a single-stage vapor-compression system including a condenser and a phase separator represented in the schematic in Figure 2.2. In S.G. Kim and M.S. Kim's (2002) design, the refrigerant mixture leaves the condenser partially condensed and enters a phase separator where it diverges into vapor and liquid streams. The liquid refrigerant mixture is expanded in an isenthalpic process to decrease the pressure and temperature, while the vapor mixture is condensed in an internal heat exchanger by the refrigerant leaving the evaporator. Both refrigerant mixture lines enter an evaporative condenser and the vapor mixture is condensed further to a saturated liquid state. The saturated liquid then is expanded through an isenthalpic expansion valve that lowers the pressure and temperature. Leaving the expansion valve, the refrigerant mixture enters the low temperature evaporator where it absorbs the heat load and exits as a superheated vapor. This refrigeration cycle design provides

improved cooling capacity while effectively utilizing a hydrocarbon, but demands increased compressor power leading to a lower COP.

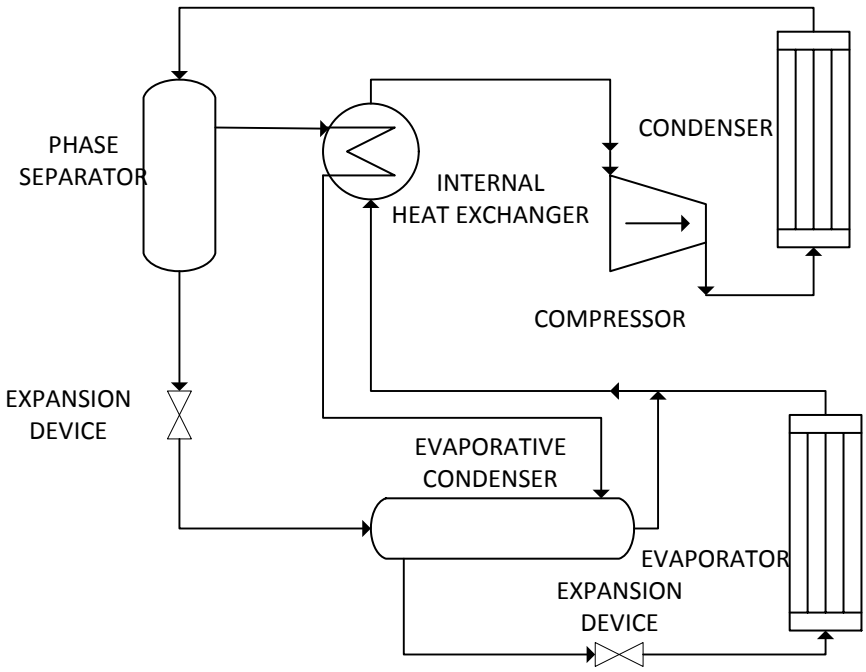

Figure 2.2: Refrigeration diagram for research by S.G. Kim and M.S. Kim (2002).

Another approach for a single-stage refrigeration system, shown in Figure 2.2, was developed by Wang, Cui, Sun and Chen (2011) based upon an auto-cascade refrigerator. A numerical study was performed in their work to optimize the compression and the composition ratio of six binary refrigerant mixtures for maximum COP. The refrigerant mixture exits the compressor, is partially condensed in an aftercooler, and then flows into a rectifying column where it is separated into a liquid and a vapor. Vapor exits the top of the column and enters two successive recuperators, where it is cooled by the expanded liquid refrigerant leaving the bottom of the rectifying column. The partially condensed liquid-vapor mixture leaving the second recuperator flows to a third recuperator (where it is fully condensed) then flows through an expansion valve to lower the pressure and temperature and finally enters the evaporator. At the exit of the evaporator, the refrigerant vapor enters the third recuperator, where it is used to fully

condense the mixture line going into the evaporator, and then mixes with the liquid line from the rectifying column. A vapor refrigerant line exits the first recuperator to send the vapor back to the compressor to continue the cycle. The research found that all of the binary refrigerant mixtures predicted COPs less than 0.5, which indicates that the cycle requires significant refinement to be feasible. However, the research illustrated that the optimum pressure ratio of the compressor must be determined first, before the composition ratio of the refrigerant.

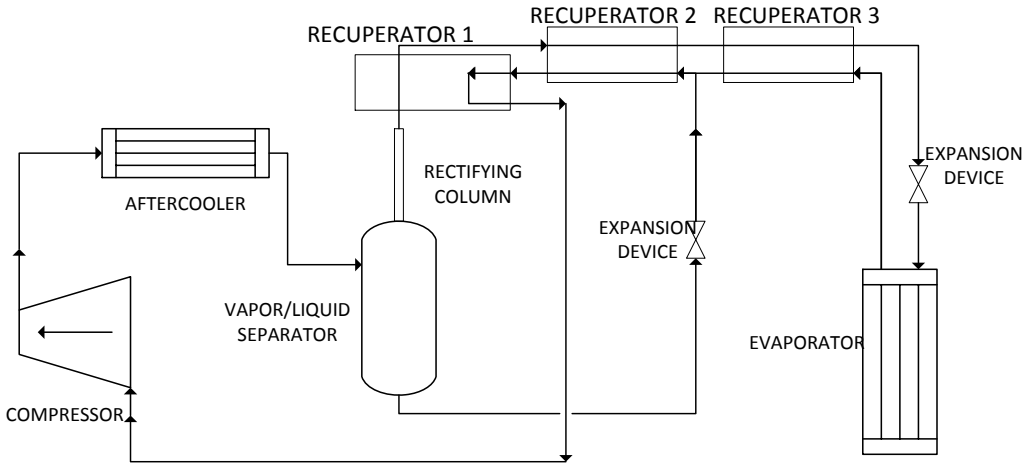

Figure 2.3: Refrigeration schematic from research by Wang et al. (2011).

The examination of binary refrigerant mixtures by S.G. Kim and M.S. Kim (2002) identified improvements that can be made to the overall refrigeration cycle. The cycle studied by Wang et al. (2011) took a similar approach, but is more complicated due to the four different heat exchangers that must be balanced to operate the refrigeration cycle.

Therefore, the proposed binary refrigerant mixture cycle prototype in this work is closer in design to Kim and Kim's apparatus but includes several modifications. It employs only one condensing separator and one brazed plate heat exchanger to be used as the inter-stage heat exchanger to condense the vapor stream from the separation column. The cycle heat is rejected to the environment as part of the separation process. Modeling of the binary refrigerant mixture cycle will provide operating points to be used for performance predictions. Experimental testing

at various operating conditions, to reach ultra low evaporator temperatures, will provide feedback in order to develop a more accurate model. The results will provide insights for improved refrigeration cycle efficiency at low temperatures as well as suggestions for future research.

2.4 Refrigerant Selection

Any fluid that exhibits advantageous thermodynamic properties while used for a direct cooling process can be considered a refrigerant. Common refrigerants used in the heating, ventilation, air conditioning and refrigeration (HVAC&R)industries are composed of halocarbons, hydrocarbons, inorganic compounds as well as blends of various compounds (Dincer, 2003). Halocarbons were increasingly used until it was determined they had harmful effects on the environment. Then hydrocarbons became the most popular refrigerant used in HVAC&R applications because they had less detrimental effects on the environment.

Before the development of refrigerant blends that provided enhanced thermodynamic properties for low temperature refrigerants, R134a and R23 were used for two-stage cascade ULT refrigeration. The R134a was used in the high stage and the R23 was used in the low stage cycles for ULT applications that could reach evaporating temperatures near -90 °C (-130 °F). Simple refrigerants, such as R134a and R23, which each consist of only one constituent, make up great binary refrigerant mixture combinations because there are only two chemical compounds that must be accounted for throughout the system. Use of simple refrigerants with well known behaviors allows for the development of a more accurate refrigeration cycle model in order to predict the operating characteristics of the system.

2.5 Mixed Refrigerant System Design Criteria

A mixed refrigerant system is designed to operate with a mixture of R23 and R134a to reach an evaporator temperature of -87 °C (-124.6 °F). At the specified evaporator temperature, a

heat load of 256.4 W (875 Btu/hr) is used to develop operating points from the mixed refrigerant cycle model. A compression ratio of 15:1 is the highest compression ratio that the Copeland CF12 compressor can practically operate on a continuously basis, such as the system capabilities will be limited by this parameter. To compare the mixed refrigerant system model to a current refrigeration cycle, a two-stage cascade refrigeration cycle will be analyzed using R23 for the low-stage and R134a for the high stage. This will provide a theoretical comparison between the cascade system and the mixed refrigerant system. Experimental results will be obtained for the mixed refrigerant system based on the operating parameters found from the system model to enhance the understanding of designing mixed refrigerant systems for ULT applications.

Chapter 3

Two-Stage Cascade Refrigeration System

A two-stage cascade refrigeration system will be used as the standard low temperature design in order to evaluate the experimental results of the mixed refrigerant system. The two-stage cascade refrigeration system will use R404A for the high stage and R508B for the low stage, which is different from the R134a and R23 mixture used in the mixed refrigerant prototype. A two-stage cascade system with an R404A/R508B combination rather than an R134a/R23 combination is evaluated to compare the mixed refrigerant system to the modern performance of a ULT system. Copeland CF series compressors (Emerson, 2010a; Emerson, 2010b) will be used for both stages in the two-stage cascade system. Although the refrigerants used are different, using the same line of compressors from Copeland will provide reasonably accurate performance comparisons to the mixed refrigerant system that also uses a Copeland CF compressor (Emerson, 2010a; Emerson, 2010b). Various evaporator temperatures and heat loads will be analyzed for the cascade system with the same reciprocating compressor setup to provide a direct comparison to the mixed refrigerant system.

A model of the two-stage cascade system is performed to determine the initial operating points and the theoretical system performance. Three operating points are analyzed at evaporator temperatures of -97 °C (-142.6 °F), -87 °C (-124.6 °F) and -82 °C (-115.6 °F) to determine the behavior of the system at increasing heat loads. Experimental results were obtained from Farrar Scientific at evaporator temperatures of -97 °C (-142.6 °F), -87 °C (-124.6 °F) and -82 °C (-115.6 °F) and applied heat loads of 507.8 W (1733.3 Btu/hr), 1128.7 W (3852.1 Btu/hr), and 1528.5 (5216.9 Btu/hr). Performance of the system is evaluated by determining the coefficient of performance (COP), Carnot COP and second law efficiency.

3.1 Refrigeration Cycle Schematic

To develop a standard model for current low temperature refrigeration, a two-stage cascade system will be analyzed. The first stage will be considered the high stage because it uses a refrigerant that has a higher boiling temperature at atmospheric pressure and the second stage, the low stage, will use a refrigerant that has a low boiling temperature at atmospheric pressure. As shown in Figure 3.1, the two-stage cascade system consists of a high-stage compressor, and, expansion device, a low-stage compressor, and expansion device, condenser, evaporator, and an inter-stage heat exchanger. The inter-stage heat exchanger functions as the evaporator of the high stage cycle and the condenser of the low stage cycle.

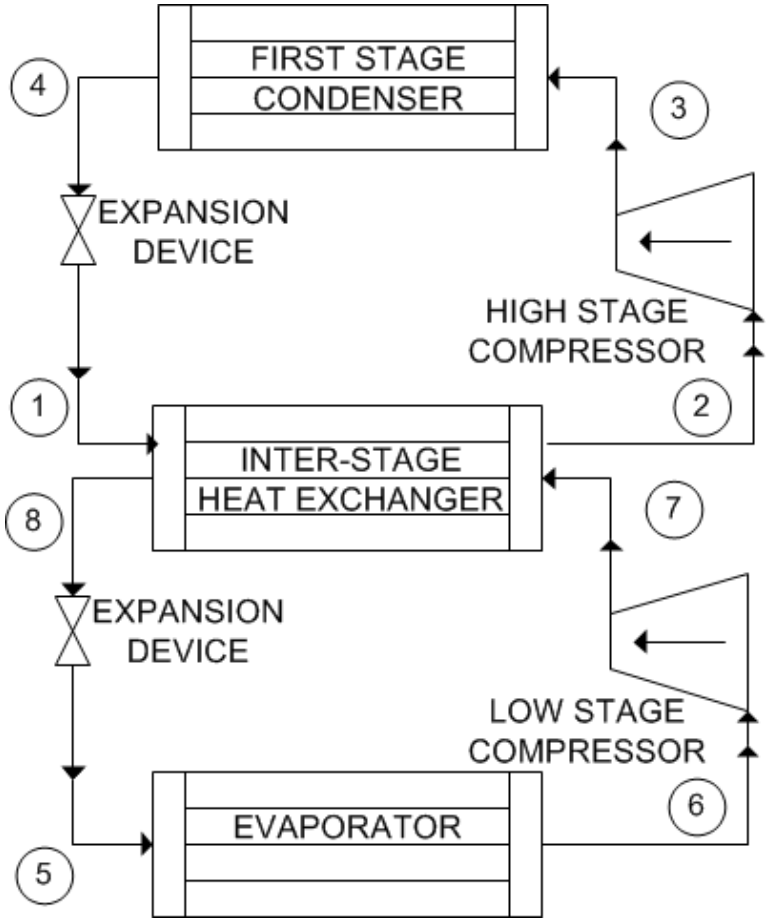

Figure 3.1: Two-stage cascade refrigeration schematic.

3.2 Refrigeration Cycle Analysis

For the two-stage cascade refrigeration system, a Copeland CF12 will provide work to the high-stage cycle and a Copeland CF09 will provide the work input to the low-stage cycle (Emerson, 2010a; Emerson, 2010b). It will be assumed that the inter-stage heat exchanger is a brazed plate heat exchanger sized appropriately from the system analysis. The condenser will be a coil and fin design typical of commercial ULT refrigeration systems. The evaporator will be a copper coil design that would be wrapped around the cabinet to efficiently absorb all of the heat from inside of the cabinet. Both of the expansion devices will be capillary tubes for this analysis because the heat load at each operating point will be selected such that the refrigerant leaving the evaporator is a saturated vapor.

3.2.1 Low-Stage Analysis

The refrigeration cycle analysis begins by specifying the design heat load and temperature requirements. A proposed storage temperature for the refrigeration system is used to determine the required evaporator temperature. The temperature required at the inlet of the evaporator must be at least 2.8 °C (5 °F) lower than the desired storage temperature to drive heat transfer from the warmer storage cabinet to the cooler refrigerant. At the outlet of the evaporator the R508B must be saturated vapor to ensure that the maximum heat load can be removed from the refrigerated space. State 6', at the evaporator exit, is defined by the suction pressure and a quality of one, shown in Figure 3.2. The desired temperature in the evaporator is used to find the saturation pressure at state 6', the suction pressure for the low-stage cycle.

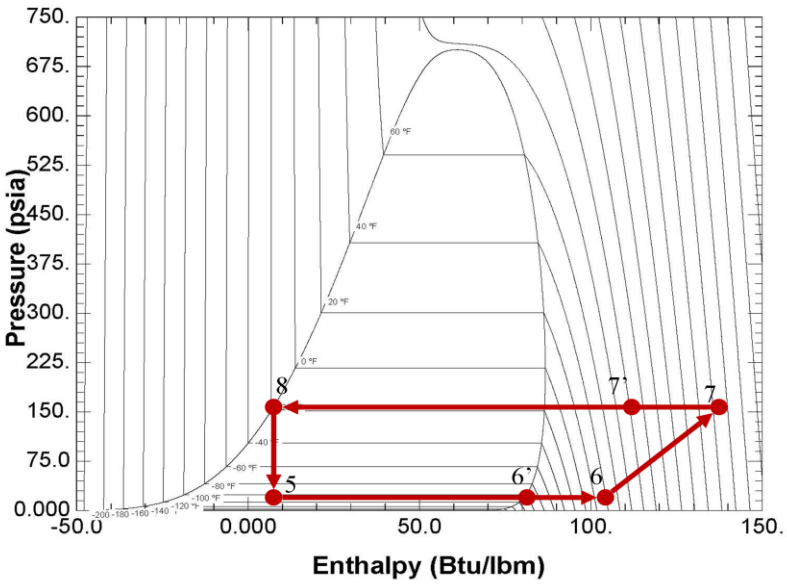

Figure 3.2: Pressure versus enthalpy diagram for R508B.

The enthalpy of the R508B leaving the evaporator can be found since the state is fixed and the enthalpy of the R508B entering the evaporator can be determined by assuming that saturated liquid leaves the inter-stage heat exchanger and expands isenthalpically. Using the first law of thermodynamics to perform an energy balance on the evaporator from state 5 to state 6' and inputting the desired heat load, the mass flow rate of the refrigerant will be determined from:

$$\dot{m}_{R508B} = \dot{Q}_{EVAPORATOR}/(h_{6'} - h_5)\,. \tag{3.1}$$

The return gas temperature specified by Copeland for the CF09 (Emerson, 2010a) used in the low-stage is 4.4 °C (40 °F), and this will be used for the temperature at state 6 entering the compressor. The suction pressure is assumed to be equal to the saturation pressure found at state 6'. Therefore, state 6 is defined by the suction pressure and the return gas temperature. In order to find the enthalpy of state 5 the enthalpy of state 8 must be found. State 8 is defined by the desired condensing temperature and a quality of zero, saturated liquid state. Knowing the enthalpy at state 8 and assuming that the expansion process is isenthalpic, the enthalpy at state 5 is equal to the enthalpy at state 8. Assuming negligible pressure drop in the condenser, the saturation pressure at state 8 will be the discharge pressure for the cycle.

The isentropic efficiency of the compressor will be used to define the actual outlet state of the compressor. It is assumed that the Copeland CF09 (Emerson, 2010a) compressor has an isentropic efficiency of 50%. The isentropic efficiency is assumed to be the lowest value from the manufacturer's data since the efficiency is shown to drop as the evaporator temperature decreases and data is not supplied for evaporator temperatures used in this research. From state 6 to state 7', the compressor follows a line of constant entropy. The discharge pressure and the compressor inlet entropy will define state 7'. Isentropic efficiency is defined as the ideal specific work divided by the actual specific work in the compressor, which simplifies to (changes in kinetic energy, potential energy and heat loss are neglected):

$$\eta_{Isentropic} = \frac{h_{7'} - h_6}{h_7 - h_6}. \tag{3.2}$$

The enthalpy at state 7 can be determined from Equation 3.2 to fix state 7, which is also at the discharge pressure. The approximate actual work required by the compressor (Equation 3.3) is defined as the mass flow rate of the refrigerant multiplied by the difference in the enthalpy from state 6 to state 7.

$$\dot{W}_{CF09} = \dot{m}_{R508B}(h_6 - h_7). \tag{3.3}$$

The heat load that must be rejected in the condenser (inter-stage heat exchanger) is found by using the first law of thermodynamics on the condenser (inter-stage heat exchanger). From the outlet of the compressor to the inlet of the condenser (inter-stage heat exchanger) the refrigerant is assumed to move to the state defined in state 7' so the heat load is found by multiplying the mass flow rate of the R508B by the difference in the enthalpies at state 7' and state 8:

$$\dot{Q}_{CONDENSER} = \dot{m}_{R508B}(h_8 - h_{7'}). \tag{3.4}$$

3.2.2 High-Stage Analysis

To determine the operating points for the high-stage cycle used in the cascade system, the condenser load from the low-stage analysis is used as the evaporator load that must be removed

from the high-stage. An evaporator temperature is chosen so that it is as least 2.8 °C (5 °F) below the condensing temperature of the low-stage refrigeration cycle to drive heat transfer. The saturated vapor state (quality of one) at the evaporator temperature will be used to find the saturation pressure. This saturation pressure will be the suction pressure for the high-stage cycle. A condensing temperature is chosen so that an air-cooled condenser can be used; the discharge pressure is found from the saturated liquid state at this temperature. This saturation pressure is the discharge pressure and it must be kept within the Copeland CF12 (Emerson, 2010b) operating limits. The remaining state points for the high-stage cycle presented in Figure 3.3 can be found using the same procedure described for the low-stage cycle analysis.

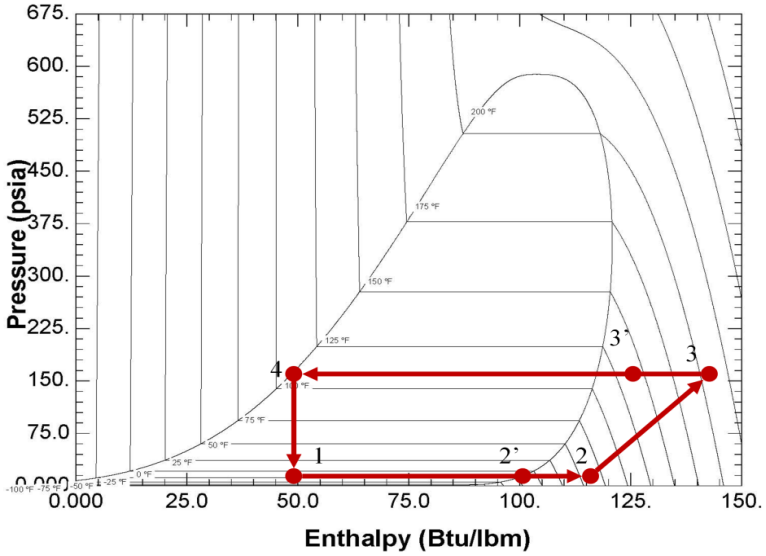

Figure 3.3: Pressure versus enthalpy diagram for R404A.

3.2.3 Cascade Model Operating Points

The two-stage cascade system model is analyzed at three specific operating points to explore how the system behaves with various heat loads and compression ratios. The heat capacity is set to 507.8 W (1733 Btu/hr), 1128.3 W (3851 Btu/hr) and 1528.6 W (5217 Btu/hr). The first analysis is performed with an evaporator capacity of 507.8 W (1733 Btu/hr) and a

suction pressure of 55.1 kPa (8.0 psia). Next, the analysis is performed with an evaporator capacity of 1128.3 W (3851 Btu/hr) and a suction pressure of 96.5 kPa (14 psia). Finally, an evaporator capacity of 1528.5 W (5217 Btu/hr) and a suction pressure of 117.2 kPa (17 psia) is analyzed.. State point results following Figure 3.1 are presented for Tests 1-3 in Appendix A. Property data presented in Tables A.1-A.3 are found using REFPROP (NIST, 2007).

3.2.4 Cascade Model Performance Analysis

The operating state points determined from the analysis of the two-stage cascade refrigeration model provide the design points for the experimental analysis. Overall performance of the cascade refrigeration model will be determined by the refrigeration capacity and the work required for the compressor. The coefficient of performance (Equation 3.5) is determined by dividing the refrigeration capacity by the overall power required by the compressor (Cengel & Boles, 2010). In the case of the two-stage cascade refrigeration system, the work required is the sum of the work for the low-stage Copeland CF09 (Emerson, 2010a) compressor and the high-stage Copeland CF12 (Emerson, 2010b) compressor.

$$COP = \frac{\dot{Q}_{Evaporator}}{\dot{W}_{CF12}+\dot{W}_{CF09}} \tag{3.5}$$

The maximum possible COP for a refrigeration cycle is the Carnot COP, which is defined in terms of the heat source and the sink temperatures as shown in Equation 3.6. The evaporator inlet temperature is used for the source temperature and the sink temperature in this case is the atmospheric air temperature. All temperatures used for the Carnot COP are in absolute units.

$$COP_{Carnot} = \frac{T_{Source}}{T_{Sink}-T_{Source}} \tag{3.6}$$

The second law efficiency of the refrigeration cycle, in Equation 3.7, is found by dividing the calculated COP of the system (Equation 3.5) by the reversible, Carnot COP (Equation 3.6). The COP, Carnot COP, and the second law efficiency are recorded in Table 3.1 for the three operating conditions analyzed for the two-stage cascade system.

$$\eta_{II} = \frac{COP}{COP_{Carnot}} \tag{3.7}$$

Table 3.1: Performance characteristics of two-stage cascade system model.

Test	1	2	3
Evaporator Inlet Temperature (°F)	-143.5	-127.1	-121.0
High-Stage C.R.	13.0	11.7	10.4
Low-Stage C.R.	13.4	9.7	9.1
Heat Load (Btu/hr)	1733.3	3852.1	5217.0
Power (Btu/hr)	4760.4	10171.2	19720
COP	0.36	0.38	0.26
Carnot COP	1.46	1.66	1.78
Second Law Efficiency (η_{II})	0.25	0.23	0.15

3.3 Experimental Two-Stage Cascade System

Experimental results were provided by the engineers at Farrar Scientific for a two-stage cascade system using a Copeland CF12 (Emerson, 2010b) for the high-stage and a Copeland CF09 (Emerson, 2010a) for the low-stage. The low-stage cycle used refrigerant 508B and the high-stage cycle used refrigerant 404A, common refrigerant combinations for ULT cascade refrigeration systems. Overall performance results for the COP, reversible Carnot COP, and second law efficiency were provided along with the evaporating temperatures for the low-stage cycle. The heat loads that were examined are identical to those used for the two-stage cascade

system model analysis in sections 3.2.3 and 3.2.4. The tests were conducted in 2006 at Farrar Scientific and the system results are provided in Table 3.2.

Table 3.2: Experimental performance characteristics of two-stage cascade system.

Test	1	2	3
Evaporator Inlet Temperature (°F)	-142.6	-124.6	-115.6
High-Stage C.R.	13.0	11.8	10.5
Low-Stage C.R.	13.3	9.8	9.0
Heat Load (Btu/hr)	1733.3	3852.1	5216.9
Power (Btu/hr)	9598.6	10643.9	11594.2
COP	0.18	0.36	0.45
Carnot COP	1.47	1.62	1.74
Second Law Efficiency (η_{II})	0.12	0.22	0.26

Chapter 4

Mixed Refrigerant System

The mixed refrigerant system will operate with a binary refrigerant mixture with work provided by a single reciprocating compressor. A water-cooled condenser will be used to separate the refrigerant mixture into two streams, a condensed liquid stream and a saturated vapor stream. The liquid stream will be expanded to a low pressure and temperature to absorb energy from the superheated vapor stream leaving the separator in order to condense it to a saturated liquid state. Once the superheated vapor stream condenses, it is expanded to a low pressure and temperature to absorb energy from the refrigerated space in the evaporator. The refrigeration schematic, refrigerant mixture properties and refrigeration cycle analysis are presented to develop a prototype apparatus.

4.1 Refrigeration Cycle Schematic

The cycle begins as the binary refrigerant mixture enters the suction side of the compressor as a superheated vapor mixture, represented by state 1 in the refrigeration schematic in Figure 4.1. Following compression, the vapor mixture enters a water-cooled condenser at state 2 and is partially condensed at constant pressure. A water-cooled condenser is employed for the separator to allow for maximum variability of the condensing properties by controlling the inlet chilled water temperature and flow rate. The separator is oriented in a vertical arrangement with the refrigerant mixture inlet above the bottom of the cylinder to allow for collection of the liquid condensate at the bottom of the separator. In the separator, heat is absorbed by the chilled water so that a portion of the refrigerant mixture can be condensed. The separator also serves as the high temperatures heat sink for the system. A mixture of R23 and R134a is condensed and exits as an R134a-heavy saturated liquid at state 3. The remaining R23 and R134a mixture that is not

condensed to a saturated liquid leaves the separator as a vapor at state 6, and this will be referred to as the R23-heavy stream. Both streams leaving the separator are a mixture of R23 and R134a; the vapor stream contains a higher percentage of R23 by mass and the liquid stream contains a higher percentage of R134a by mass.

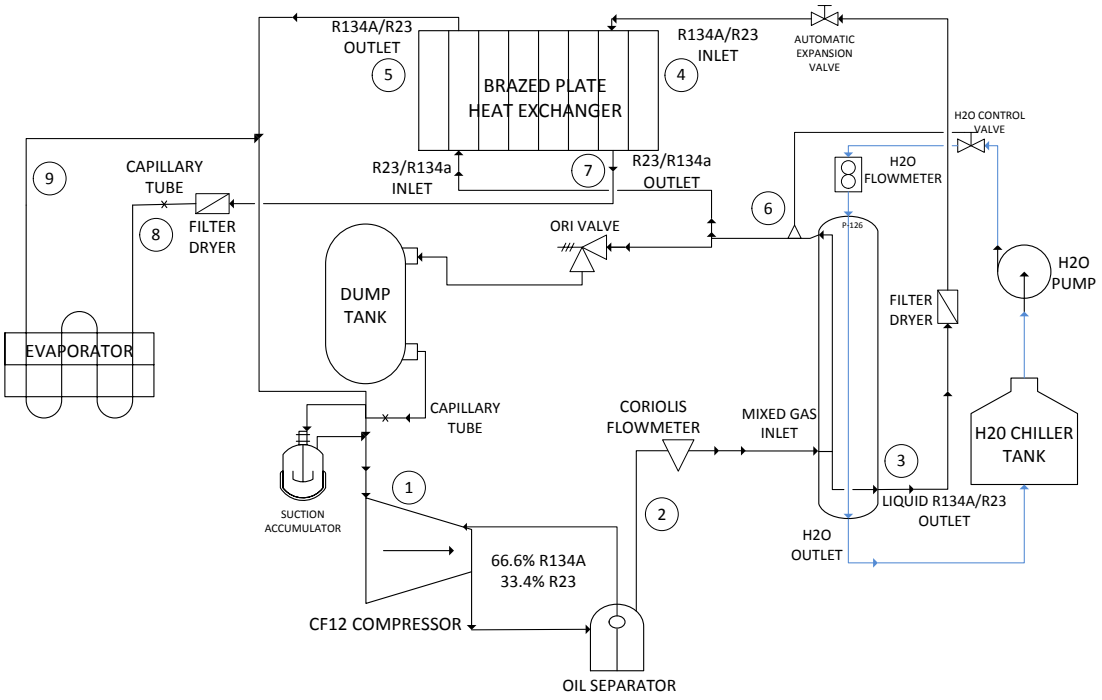

Figure 4.1: Mixed refrigerant system schematic.

The R134a-heavy stream leaves the separator as a saturated liquid and it enters an expansion device that decreases the pressure and subsequently the temperature of the mixture. It then enters a brazed plate heat exchanger (BPHE) as a two phase liquid-vapor mixture at state 4, as shown in Figure 4.1. The R23-heavy stream leaves the separator at state 6 and enters the BPHE as a slightly superheated vapor. Energy rejected by the R23-heavy stream is absorbed by the R134a-heavy stream that has been expanded to a low pressure. The R134a-heavy stream exiting the BPHE at state 5 is assumed to have completely evaporated to a saturated vapor with a quality of one. Advancing towards the compressor, the R134a-heavy vapor will slightly

superheat due to the temperature difference with the surrounding air, thus making sure there is no liquid entering the suction side of the compressor. The R134a-heavy stream will be re-mixed with the R23-heavy stream prior to entering the suction side of the compressor.

The BPHE acts similar to an inter-stage heat exchanger for a typical cascade refrigeration system. Exiting the heat exchanger at state 7, the R23-heavy stream is assumed to be completely condensed to a saturated liquid. Then the R23-heavy stream flows through an expansion device in an isenthalpic process to drop the pressure and therefore the temperature to state 8. Five hollow, rectangular plates with a combined length of 80 feet of embedded horizontal copper tubing are connected in series and stacked upon one another to serve as the evaporator. Silicone heating sheets in between each evaporator plate supply a nearly constant heat load representing the energy that must be removed by the refrigerant mixture. The R23-heavy stream evaporates as it moves along the copper tubing of the evaporator, absorbing the energy provided by the silicone heating sheets. Exiting the evaporator at state 9, in Figure 4.1, the R23-heavy stream is re-combined with the R134a-heavy stream headed toward the suction side of the compressor. The two R23 and R134a mixture streams thoroughly mix and absorb some energy from the surrounding higher temperature ambient air to provide a superheated vapor mixture into the suction side of the compressor at state 1, thus completing the cycle.

4.2 Refrigerant Mixture Properties

Modeling and testing of the mixed refrigerant system is undertaken to develop a thorough understanding of the differences between theoretical and actual operation. Simple, well understood refrigerants each with one constituent only are chosen for the mixture to develop an underlying theoretical model of the cycle operation that can later be applied to more complex refrigerants. Thermo-physical properties for the mixed refrigerants are found using REFPROP Version 8.0 and Engineering Equation Solver Version 8.889 (NIST 2007; F-Chart Software 2011). Analysis of the system assuming complete separation of the two refrigerants in the

separator will be used to select an initial mixture ratio for the refrigerants to be used in experimental operation.

4.2.1 Chosen Refrigerants

The mixed refrigerant system will operate with a binary mixture of refrigerant 134a (R134a) and refrigerant 23 (R23). R134a is a hydrofluorocarbon refrigerant made of the compound 1,1,1,2-Tetrafluoroethane, produced by Dupont (Dupont,2004), and is commonly used in refrigerant cooling applications above 0 °C (32 °F). A pressure versus enthalpy diagram of R134a is presented in Figure 4.2 to show the shape of the saturation dome.

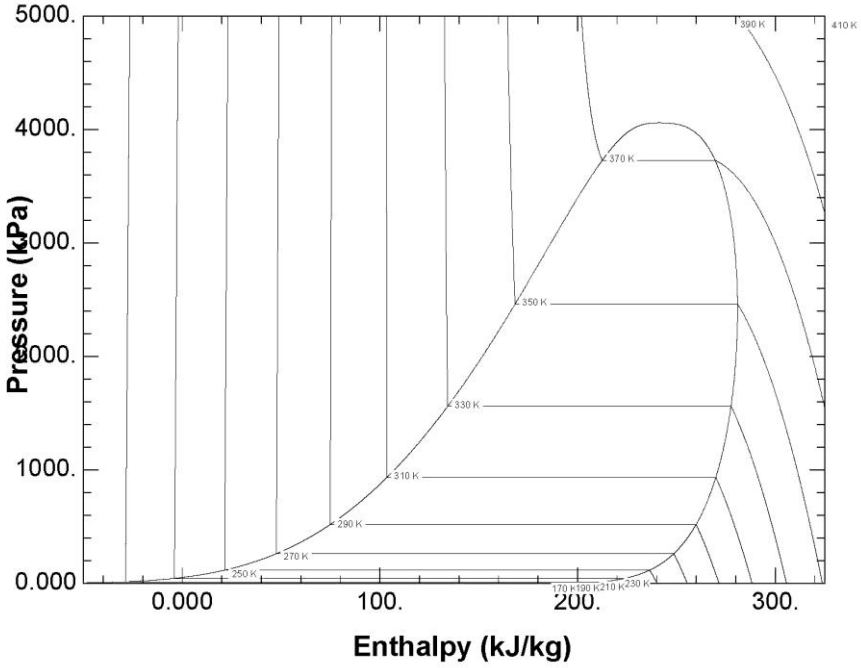

Figure 4.2: Pressure versus enthalpy diagram for R134a.

R23 is a hydrofluorocarbon refrigerant made of the compound Trifluoromethane, produced by Dupont (Dupont, 1994) and is used for low temperature refrigeration well below 0 °C (32 °F) due to its low critical point. A pressure versus enthalpy diagram of R23 is presented

in Figure 4.3 to show the shape of the saturation dome and the location of the critical point properties.

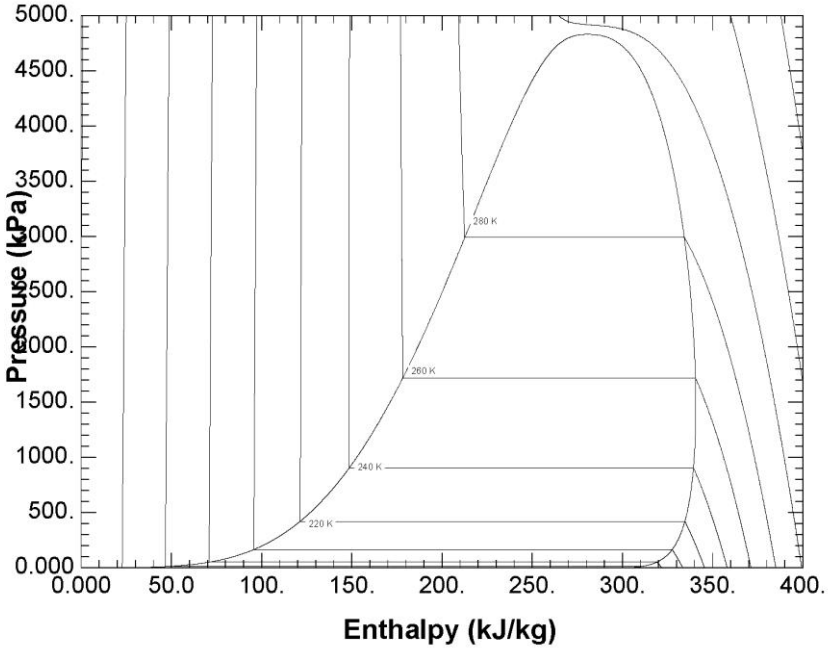

Figure 4.3: Pressure versus enthalpy diagram for R23.

The refrigerant mixture of R23 and R134a will be separated into two separate streams in a condenser. Perfect separation of the R23 from the R134a will not occur in the condensing separator at the operating conditions the mixed refrigerant system, therefore, the vapor stream and the liquid stream leaving the separator will be a mixture of both R23 and R134a. A binary phase diagram for a refrigerant mixture of 33.4% R23 and 66.6% R134a is shown in Figure 4.4 at the discharge pressure of 1137.6 kPa (165 psia) to illustrate the resulting composition ratios of the liquid and vapor mixtures leaving the separator. REFPROP Version 8.889 (NIST, 2007) is used to determine the refrigerant mixture properties at each specified state point for the mixed refrigerant system.

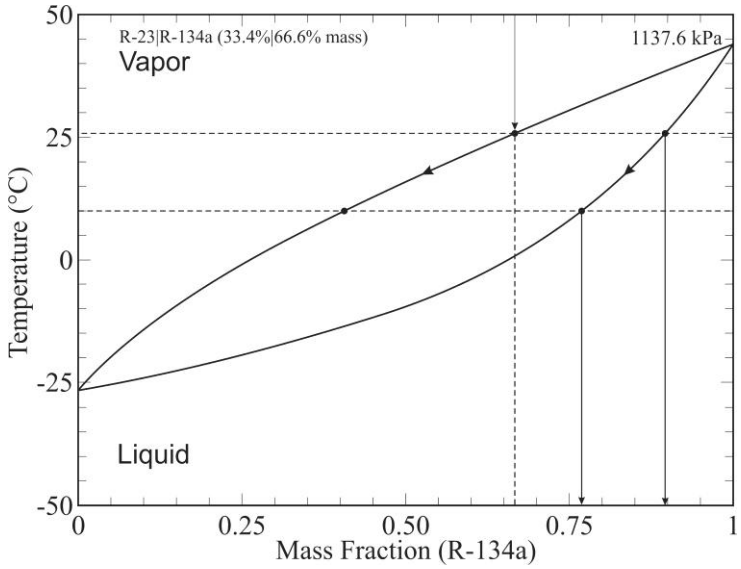

Figure 4.4: Phase diagram, 33.4% R23 and 66.6% R134a by mass at 1137.6 kPa (165 psia) (NIST, 2007).

4.2.2 REFPROP Refrigerant Properties

All refrigerant properties are found using the ASHRAE reference state, entropy and enthalpy of zero for saturated liquid at -40 °C (-40 °F). Refrigerant mixtures will be defined by percentage mass since the system will be charged with refrigerants measured by weight. The screen capture from REFRPROP provided in Figure 4.5 shows how the refrigerant mixture is defined under Substance -> Define New Mixture.

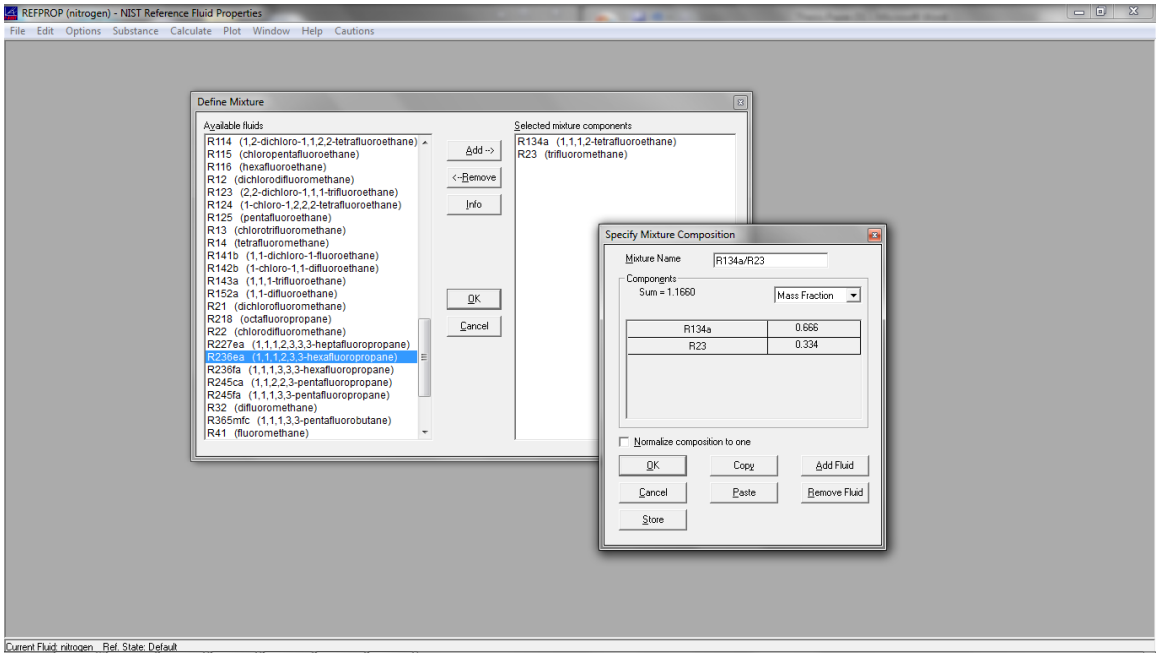

Figure 4.5: Defining new mixture in REFPROP by mass percentage (NIST, 2007).

Once the mixture is defined, two independent properties are required to specify a state point and all other properties can be found. REFPROP (NIST, 2007) can also be used to produce binary phase diagrams for refrigerant mixtures. Therefore, REFPROP (NIST, 2007) will be used to look up properties for the analysis of the mixed refrigerant system and diagrams will be produced to illustrate the operating range of the mixtures.

In order to begin the analysis of the mixed refrigerant system, an initial mixture ratio must be determined from the initial system design parameters. To determine the overall mixture ratio of R23 to R134a, the mixed refrigerant cycle will be analyzed assuming perfect separation, with two separate streams of R23 and R134aexiting the condensing separator.

4.2.3 Binary Refrigerant Mixture Ratio

Once the two refrigerants are separated into independent streams, the mixed refrigerant system behaves like a cascade cycle; the low-stage R23 is condensed by the high-stage R134a in an inter-stage heat exchanger and absorbs the heat load in the evaporator to provide cooling. An

evaporator temperature of -87 °C (-124.6 °F) is specified for the low-stage R23 and an evaporator load of 256.4 W (875 Btu/hr) is the desired heat load to be absorbed. The suction pressure is the saturation pressure at -87 °C (-124.6 °F) and a compression ratio of 15:1 will be used to determine the discharge pressure once the saturation pressure at -87 ° C (-124.6 °F) identifies the suction pressure in the evaporator because the ratio is reasonable for the compressor line used in this application.

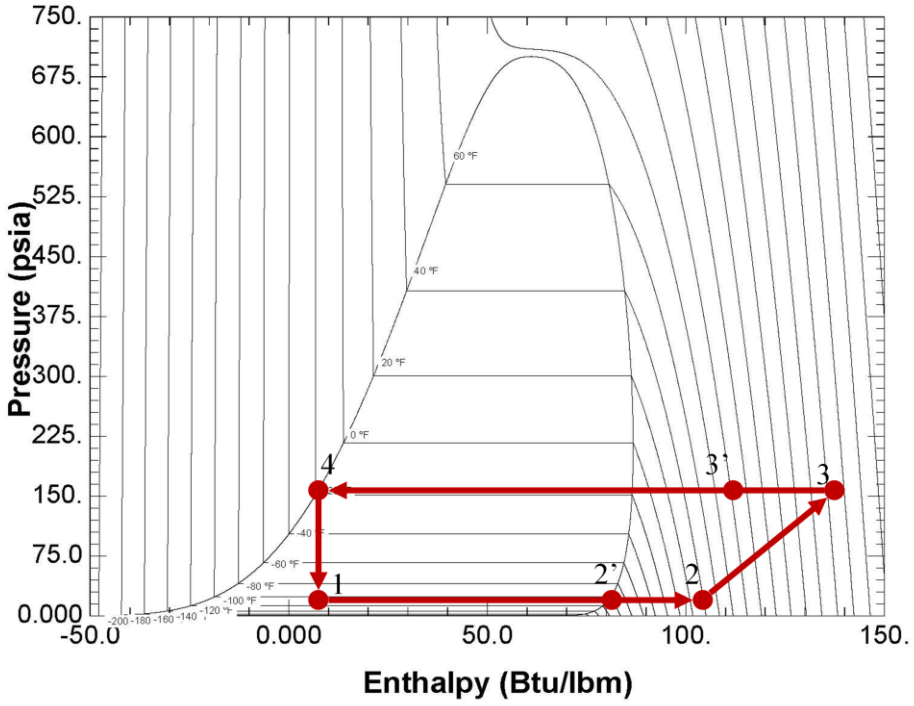

Figure 4.6: Pressure versus enthalpy diagram for R23.

In order to determine the amount of R23 required to remove the desired heat load from the evaporator, state 1 to state 2 prime in Figure 4.6, an energy balance is performed. The energy balance on the evaporator (Equation 4.1) illustrates that the heat load to be removed from the evaporator is equal to the mass flow rate of the R23 multiplied by the difference between the enthalpy of the R23 leaving the evaporator at state 2' and the enthalpy of the R23 leaving the expansion valve at state 1. By specifying the heat load absorbed in the evaporator, the mass flow rate of the R23 can be found.

$$\dot{m}_{R23} = Q_{EVAP}/(h_{2'} - h_1) \quad (4.1)$$

The expansion device is assumed to be isenthalpic, so the enthalpy of the R23 leaving the expansion device at state 1 is equal to the enthalpy entering the expansion device at state 4. The R23 leaving the condenser is assumed to be a saturated liquid so the enthalpy of the R23 entering the expansion valve, state 1, is found by specifying state 4 with a quality of zero and the discharge pressure. At the outlet of the evaporator, the enthalpy is found by assuming the last amount of R23 evaporates just as it leaves the evaporator and it is a saturated vapor. Leaving the evaporator, the R23 at state 2' in Figure 4.6 is specified by a quality of one and the suction pressure.

As the R23 vapor leaves the evaporator, it absorbs some energy from state 2' until it reaches state 2 where it enters the compressor. In this work, the compressor inlet temperature is assumed to be 4.4 °C (40 °F) to be consistent with the compressor performance data, so that the deviation in the compressor efficiency is similar. The R23 will be mixed with the R134a superheated vapor and enters the compressor, which operates between states 2 and 3, leaving the mixture as a superheated vapor form at the discharge. After the refrigerant mixture leaves the compressor it will enter the condensing separator. The separator is assumed to condense the R134a into a saturated liquid at 37.8 °C (100 °F) and it will be assumed that the R23 is a saturated vapor at this temperature. A condensing temperature of 37.8 °C (100 °F) is chosen because it is a common condensing temperature used for two-stage cascade systems that are currently designed with air-cooled condensers. The R23 remains in vapor form and enters the brazed plate heat exchanger at 100 °F.

The R23 vapor will be condensed in the brazed plate heat exchanger. At the exit of the separator the R23 is assumed to be at the discharge pressure and the condensing temperature of 100 °F which leaves the R23 in a superheated vapor state. An energy balance (Equation 4.2) is performed on the R23 in the condenser to determine the heat load that must be dissipated in the brazed plate heat exchanger.

$$\dot{Q}_{Condenser} = \dot{m}_{R23}(h_4 - h_{3'}) \tag{4.2}$$

The heat load removed from the R23 to condense it to a saturated liquid must equal the amount of heat the inter-stage heat exchanger can remove by the R134a. A diagram of the refrigeration cycle for the R134a is presented in Figure 4.7.

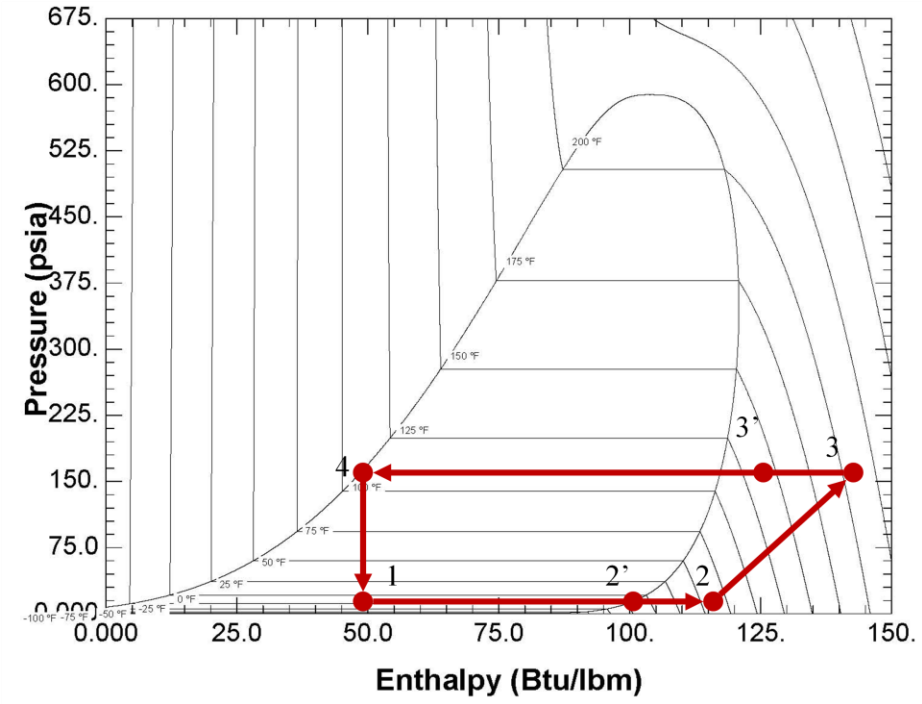

Figure 4.7: Pressure versus enthalpy diagram for R134a.

Because the heat removed by the R134a in the inter-stage heat exchanger is known, the first law of thermodynamics is used to perform a heat balance on the R134a as it evaporates from state 1 to state 2' in Figure 4.7:

$$\dot{m}_{R134a} = \dot{Q}_{Evap,R134a}/(h_{2'} - h_1). \tag{4.3}$$

State 1 is defined by the suction pressure and the enthalpy of the R134a entering the expansion device, assuming isenthalpic expansion. The enthalpy of R134a entering the expansion device at the discharge pressure is found assuming the refrigerant is a saturated liquid at the outlet of the condenser with a quality of zero. Through the expansion device, the

refrigerant is expanded to a low pressure and temperature in an isenthalpic process, leaving the enthalpy at the entrance of the evaporator equal to that entering the expansion device.

The mass flow required for the R134a can be found from Equation 4.3. Summing the mass flow rate of R23 and R134a required will determine the overall mass flow rate in the compressor. Dividing the mass flow rate of the R23 and that of the R134a by the total flow rate gives the refrigerant ratio by mass, represented in the following Equations 4.4 and 4.5.

$$X_{R23} = \frac{\dot{m}_{R23}}{\dot{M}_T} \qquad X_{R134a} = \frac{\dot{m}_{R134a}}{\dot{M}_T} \qquad (4.4, 4.5)$$

4.3 Prototype Apparatus

The mixed refrigerant system (MRS) prototype apparatus was constructed by engineers and technicians at Farrar Scientific following the refrigeration diagram in Figure 4.1. A cooling system is used to provide a chilled water/glycol mixture for heat removal in the condenser-separator. The cooling system consists of a refrigeration cycle to chill the water/glycol mixture, a pump to supply the desired flow rate, and a control to set the mixture. The refrigeration cycle components are attached to a wood pallet for both stability and ease of mobility. The evaporator is built into an insulated container on the wood pallet to minimize the energy that will leave the heating pads to the environment rather than enter the evaporator. Figure 4.8 is a picture of the entire mixed refrigeration system.

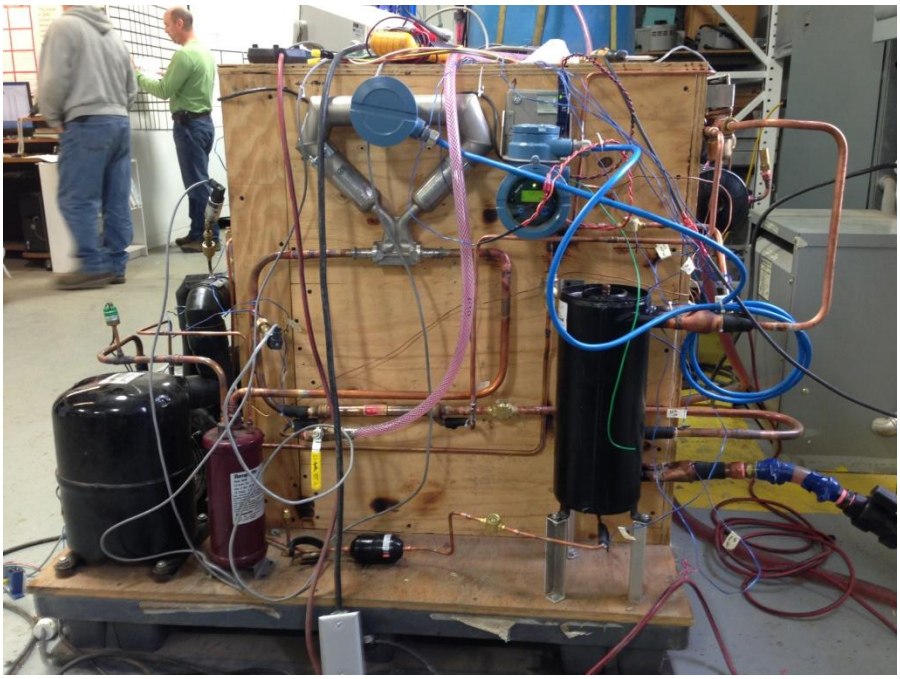

Figure 4.8: Mixed refrigerant system apparatus.

4.4 Mixed Refrigerant Cycle Analysis

The initial model, assuming perfect separation, was used to select a refrigerant composition. The model was then modified to consider imperfect separation and better predict the behavior of the MRS under operation. The model is used for two main purposes: to determine the operating points and predicted performance of the system, and to analyze the performance of the system under specified operating conditions. Initially the model of the MRS is used to find the operating parameters that will fulfill the desired design characteristics. Then, testing is performed to determine the experimental behavior of the MRS. Once the experimental results are obtained, the MRS model is used to analyze the components to develop an understanding of the operation behavior of the system.

Predicted performance and operational behavior of the MRS will be defined by state points throughout the system. State points in the MRS are determined by the position of the components that can be found in the refrigeration diagram in Figure 4.1. All state points for the

model analysis are assumed to be operating at a steady state condition. Model analysis begins at the compressor where the refrigerant mixture ratio is assumed to be the initial refrigerant mixture charge by mass. Next, a mass balance is performed on the separator to determine the mass flow rate and the refrigerant mixture ratio of the two streams leaving the separator. Each refrigerant mixture stream is used to analyze the operating points and performance of the brazed plate heat exchanger. After the brazed plate heat exchanger, the R23-heavy stream is analyzed in the evaporator. The various state points used in the MRS model will follow the numbering convention in Figure 4.1.

4.4.1 Condensing Separator

To begin the analysis of the condensing separator, the refrigerant mixture ratio leaving the compressor is assumed to be the input refrigerant mixture ratio. The suction pressure is set from the needle valves for the R134a-heavy line entering the brazed plate heat exchanger. The discharge pressure is set by the temperature and flow rate of the chilled water/glycol used to remove energy in the separator. Modeling the mass flow rate through the separator on a per pound basis allows the determination of the mass of the total mass flow rate of the R23 and R134a refrigerants through the separator. The total mixed refrigerant mass flow rate is assumed to be one pound per hour and is multiplied by the ratio of R134a (X_{R134a}) and R23 (X_{R23}) in the MRS to find the total mass flow rate of R134a and R23 in the compressor.

$$\dot{m}_{R134a,TOTAL} = X_{R134a} * \dot{M}_{TOTAL} \tag{4.6}$$

$$\dot{m}_{R23,TOTAL} = X_{R23} * \dot{M}_{TOTAL} \tag{4.7}$$

A temperature at the condenser exit is found based on the, initial refrigerant mixture ratio and the desired discharge pressure. The initial refrigerant mixture ratio of R23 and R134a is entered into REFPROP and a pressure versus enthalpy diagram is produced in Figure 4.9 (NIST, 2007). The red line in Figure 4.9 signifies the constant pressure condensing process that is

modeled in the condensing separator. The constant temperature lines indicate that the saturated vapor temperature at constant pressure is not equal to the saturated liquid temperature. To determine the condensing temperature in the separator the saturated vapor temperature and the saturated liquid temperature at the discharge pressure conditions are found. The condensing temperature for the discharge conditions is assumed to be the average temperature between the saturated vapor temperature and the saturated liquid temperature.

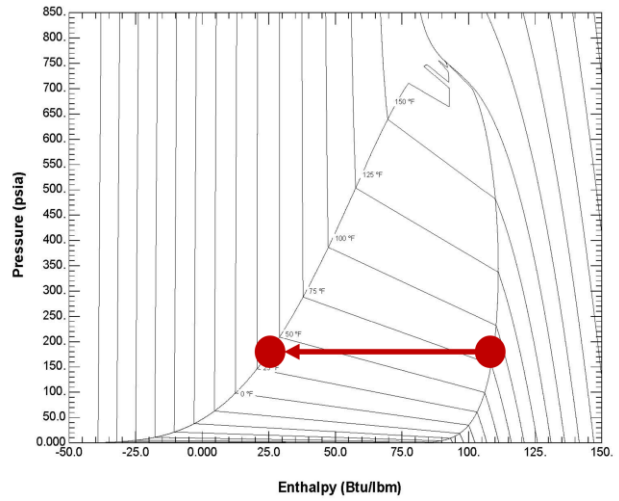

Figure 4.9: Pressure versus enthalpy diagram for 33.4% R23 and 66.6% R134a (NIST, 2007).

The saturated liquid properties are found from REFPROP (NIST, 2007) using the discharge pressure and the assumed condensing temperature in the separator. The condensing process is assumed to be a constant pressure process; therefore, the binary phase diagram from Figure 4.4 is used to represent the saturation properties at a particular condensing temperature. The phase diagram is developed assuming a constant pressure and presents the ratio of R134a increasing from 0 to 1 along the x-axis as the temperature increases along the y-axis.

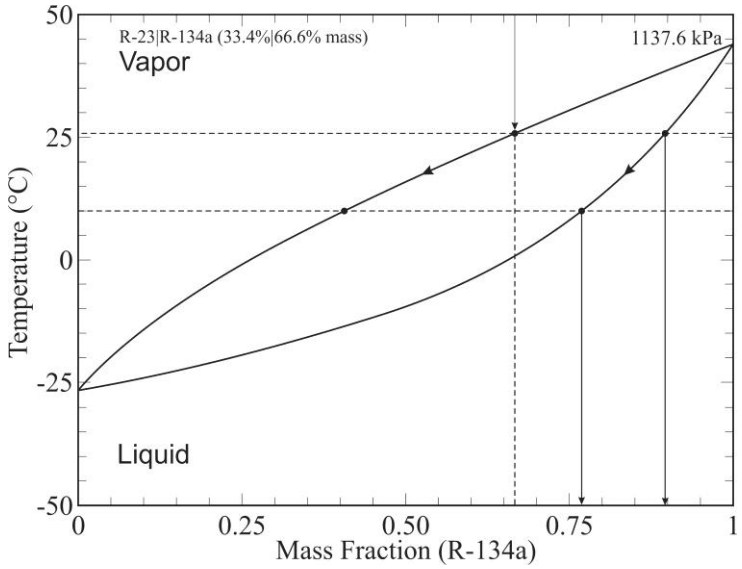

Figure 4.4: Phase diagram, 33.4% R23 and 66.6% R134a by mass at 1137.6 kPa (165 psia) (NIST, 2007).

The assumed condensing temperature at the exit of the separator is represented by the constant line at 10 °C (50 °F). At a particular condensing temperature and pressure there is a corresponding saturated liquid mass fraction of R134a ($X_{R134a,l}$) and R23 ($X_{R23,l}$) that is found in REFPROP (NIST, 2007). The resulting mass fraction will be the refrigerant mixture ratio of the saturated liquid leaving the bottom of the separator. It will consist of a higher fraction of R134a; therefore, it will be referred to as the R134a-heavy mixture.

The total mass flow rates of each of the R134a and R23 in the separator found from Equations 4.6 and 4.7 are used to determine the mass flow rate of the saturated liquid mixture ratio. Along with the mass fraction of the saturated liquid at the discharge pressure and the condensing temperature the saturated vapor mass fraction of R134a ($X_{R134a,v}$) and R23 ($X_{R23,v}$) can be found from REFPROP (NIST, 2007). The mass flow rate of the saturated liquid R134a and R23 can be determined from Equations 4.8 and 4.9.

$$\dot{m}_{R134a,l} = X_{R134a,l}\left(\frac{\dot{m}_{R134a,TOTAL}}{X_{R134a}}\right)\left(\frac{X_{R134a}-X_{R134a,v}}{X_{R134a,l}-X_{R134a,v}}\right) \tag{4.8}$$

$$\dot{m}_{R23,l} = X_{R23,l}\left(\frac{\dot{m}_{R23,TOTAL}}{X_{R23}}\right)\left(\frac{X_{R23}-X_{R23,v}}{X_{R23,l}-X_{R23,v}}\right) \tag{4.9}$$

The total mass flow rate of the liquid R134a-heavy stream is found by summing the mass flow rates from Equations 4.8 and 4.9.

$$\dot{m}_{Liquid,TOTAL} = \dot{m}_{Liquid,R134a} + m_{Liquid,R23} \tag{4.10}$$

The mass flow rates of the R134a and R23 in a vaporous state are found by subtracting the mass flow rates in equation 4.8 and 4.9 from the total mass flow rates in equation 4.6 and 4.7.

$$\dot{m}_{R134a,v} = \dot{m}_{R134a,TOTAL} - \dot{m}_{R134a,l} \tag{4.11}$$

$$\dot{m}_{R23,v} = \dot{m}_{R23,TOTAL} - \dot{m}_{R23,l} \tag{4.12}$$

The total mass flow rate for the vapor refrigerant mixture is found by summing Equations 4.11 and 4.12

$$\dot{m}_{Vapor,TOTAL} = \dot{m}_{R134a,v} + \dot{m}_{R23,v}. \tag{4.13}$$

At the exit of the separator, the vaporous refrigerant mixture ratio can be found by dividing the mass flow rates for the R134a and R23 in equations 4.11 and 4.12, respectively, by the total mass flow rate from Equation 4.13. The total mass flow rate for the R23-heavy vapor stream and the R134a-heavy liquid stream is used for the mass flow rates throughout the rest of the mixed refrigerant system analysis.

4.4.2 Brazed Plate Heat Exchanger

Once the two mass flow rates and their mixture ratios are found for the lines leaving the separator, an energy balance is performed on the brazed plate heat exchanger. This is done to determine if the R134a-heavy mixture can remove enough energy to condense the R23-heavy mixture to a saturated vapor. An analysis on the brazed plate heat exchanger will provide evaporating and condensing temperatures to develop an understanding of the performance level of the heat exchanger at particular operating conditions. A piping diagram for the R23-heavy and R134a-heavy refrigerant mixture streams is presented in Figure 4.10 to illustrate the direction of heat transfer.

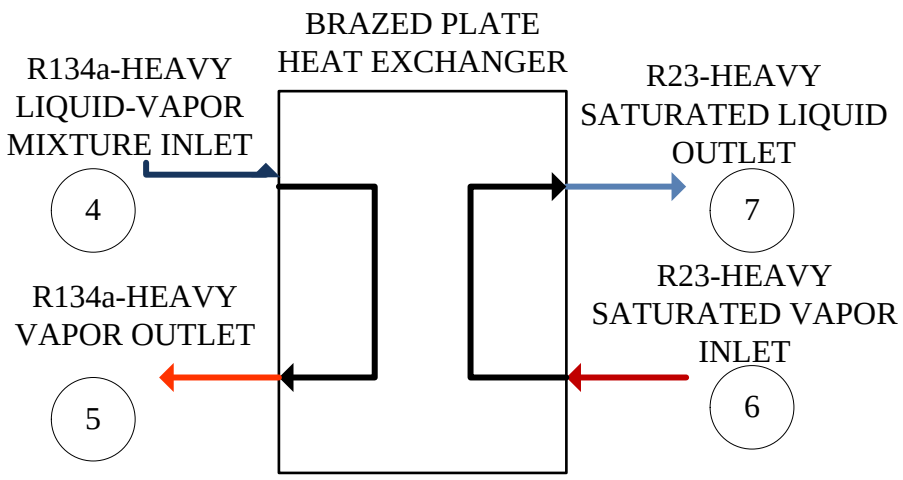

Figure 4.10: Brazed plate heat exchanger piping diagram.

An energy balance is performed on the R23-heavy refrigerant mixture using the first law of thermodynamics. The amount of heat that must be dissipated to condense the R23-heavy refrigerant mixture to a saturated liquid is found by multiplying the mass flow rate in Equation 4.13 by the difference in the enthalpies from state 6 to state 7.

$$\dot{Q}_{BPHE,R23} = \dot{m}_{Vapor,TOTAL}(h_7 - h_6) \tag{4.14}$$

The enthalpy at state 6 is found using the condensing temperature that is assumed for the separator exit and the discharge pressure that is set the compressor outlet conditions. Since state 6 is a binary mixture, these three independent properties are required to specify the state. It is assumed that the R23-heavy vapor mixture is fully condensed at the outlet of the brazed plate heat exchanger. Thus, state 7 is s saturated liquid with a quality of zero at the discharge pressure.

The R134a-heavy refrigerant mixture leaves the separator as a saturated liquid and travels to an expansion valve. The expansion valve is a needle valve set to maintain the desired suction pressure. Through the expansion valve, the refrigerant mixture is expanded to a low pressure, and therefore, low temperature. Entering the evaporator (brazed plate heat exchanger), the R134a-heavy mixture is at the suction pressure. An energy balance is performed on the R134a-heavy mixture from states 4 to 5. The amount of energy that can be removed by the R134a-heavy

mixture is found by multiplying the mass flow rate by the difference in the enthalpies from state 4 to state 5 in Equation 4.15.

$$\dot{Q}_{BPHE,R134a} = \dot{m}_{Liquid,TOTAL}(h_5 - h_4) \tag{4.15}$$

The expansion process is assumed to be an isenthalpic one and therefore the enthalpy at the outlet of the expansion valve, state 4, is equal to the enthalpy at the inlet, state 3. At the condensing separator outlet, the R134a-heavy mixture leaves as a saturated liquid, therefore state 3 is defined by the discharge pressure and a quality of zero. The enthalpy found at state 3 is equal to the enthalpy at state 4. At the exit of the evaporation process the R134a-heavy refrigerant mixture is assumed to be a saturated vapor with a quality of one. Through the evaporator the R134a-heavy mixture is at the suction pressure and the known quality defines state 5 so the enthalpy can be determined.

The energy absorbed by the R134a-heavy stream is calculated and compared to the energy that must be removed to condense the R23-heavy stream. The R134a-heavy stream must provide enough energy absorption capacity to condense the R23-heavy. The refrigeration capacity in the evaporator is thereby reduced because the R23-heavy refrigerant mixture is not completely condensed to a saturated liquid.

4.4.3 Evaporator

The evaporator is analyzed in the mixed refrigerant system model to determine the refrigeration capacity and the specific state point properties. An energy balance is performed using the first law of thermodynamics for the R23-heavy refrigerant mixture in the evaporator from state 8 to state 9. The energy that can be removed from the refrigerated space is found by multiplying the mass flow rate found from Equation 4.13 by the difference between the enthalpies from state 8 to state 9 (see Figure 4.1).

$$\dot{Q}_{Evaporator} = \dot{m}_{Vapor,TOTAL}(h_9 - h_8) \tag{4.16}$$

Exiting the brazed plate heat exchanger, the R23-heavy mixture flows through a capillary tube to expand the mixture to the suction pressure and decrease the temperature. The expansion process is assumed to be isenthalpic so the enthalpy entering the capillary tube is equal to the enthalpy at the exit. At the exit of the brazed plate heat exchanger the refrigerant mixture is a saturated liquid, so state 7 is defined by a quality of zero and the discharge pressure. The enthalpy can be found at state 7 because the state is fixed by the two independent properties. At the outlet of the evaporator, the R23-heavy mixture is assumed to be a saturated vapor with a quality of one. The discharge pressure and the quality define state 9; therefore, the enthalpy can be determined and the evaporator capacity can be calculated.

4.5 Cycle Operating Points

The mixed refrigerant system (MRS) operating points are determined from the analysis of the cycle model to provide investigation parameters for the experimental analysis. The model is run with two separate compression ratios and at two different suction pressures to predict the experimental performance of the refrigeration system. An initial suction pressure is chosen by determining the saturation pressure for R23 at an evaporating temperature of -87 °C (-124.6 °F). This suction pressure would provide the desired evaporator operating temperature for the mixed refrigeration system. For this system it is known that perfect separation will not occur , but setting the suction pressure equal to the R23 saturation pressure at -87 ° C (-124.6 °F) provides an initial starting point for analysis of the mixed refrigerant system.

The saturation pressure for R23 at -87 ° C (-124.6 °F) is found from thermofluid property data from Dupont and REFPROP (Dupont, 1994; F-Chart Software 2011) to be 75.8 kPa (11 psia). The analysis of the mixed refrigeration system is used to define all of the state points represented in the refrigeration diagram in Figure 4.1. The cycle begins as the initial refrigerant mixture ratio of R23 and R134a enters the suction side of the compressor. It will be assumed for the system model that the refrigerant mixture enters the suction side of the compressor at 4.4 °C

(40 °F). From the mixture ratio, suction pressure and temperature entering the suction side of the compressor, state 1 is defined. The outlet of the compressor, state 2, is defined by the discharge pressure and the enthalpy that can be determined from the isentropic efficiency of the Copeland CF12 compressor (Emerson, 2010). The isentropic efficiency for the compressor is assumed to be 50%. The enthalpy at the outlet of the compressor is determined from the isentropic efficiency, which is the ideal power required in the compressor divided by the actual power required:

$$\eta_{Isentropic} = \frac{h_{3\prime} - h_2}{h_3 - h_2} . \tag{4.17}$$

The remainder of the state points are determined using the analysis in section 4.4 and the results are presented in the following tables. The specific entropy at each state point is also found. A summary of the experimental testing parameters are presented in the Table 4.1. The model state point results corresponding to Figure 4.1 can be found in Appendix B for Tests 1-6.

Table 4.1: Summary of testing parameters for MRS.

Test	Overall Mixture Ratio	C.R.	Suction Pressure
1	66.6% R134a|33.4% R23	15:1	11 psia
2	66.6% R134a|33.4% R23	12:1	11 psia
3	66.6% R134a|33.4% R23	15:1	14 psia
4	66.6% R134a|33.4% R23	12:1	14 psia
5	60% R134a|40% R23	15:1	11 psia
6	60% R134a|40% R23	12:1	11 psia

4.6 Cycle Performance Analysis

The operating parameters are determined from the mixed refrigerant model described in sections 4.4-4.5 for various design points. The power consumption and the evaporating refrigeration capacity is based on determine the overall coefficient performance of the mixed refrigerant system model. Refrigeration capacity is found from Equation 4.16 and power

consumption of the compressor is determined by multiplying the mass flow rate of the initial refrigerant mixture by the difference in the enthalpies from state 2 to state 3. The overall system performance is defined using the coefficient of performance (COP); that is the refrigeration capacity divided by the compressor power consumption (Cengel & Boles, 2010).

$$COP = \frac{\dot{Q}_{Evaporator}}{\dot{W}_{Compressor}} \tag{4.18}$$

The maximum possible COP for a refrigeration cycle is the Carnot COP, which is defined in terms of the heat source and the sink temperatures as shown in Equation 4.19. For the Carnot COP the sink temperature is the condenser determined for the separator. The source temperature for the Carnot COP is the temperature of the R23-heavy refrigerant mixture entering the evaporator at state 8.

$$COP_{Carnot} = \frac{T_{Source}}{T_{Sink} - T_{Source}} \tag{4.19}$$

The second law efficiency of the refrigeration cycle, in Equation 4.20, is found by dividing the calculated COP of the system (Equation 4.18) by the reversible, Carnot COP (Equation 4.19).

$$\eta_{II} = \frac{COP}{COP_{Carnot}} \tag{4.20}$$

The evaporating temperature will be the coldest at the entrance of the evaporator so the temperature at state 8 is recorded along with the COP, Carnot COP and second law efficiency for the operating points in section 4.5. Tables 4.2 and 4.3 show the above performance parameters for the operating state points in section 4.5.

Table 4.2: Performance characteristics of model at suction pressure and compression ratio (66.6% R134a and 33.4% R23).

Suction Pressure (psia)	Compression Ratio	Evaporator Temperature (°F)	COP	Carnot COP	Second Law Efficiency (η_{II})
11.0	15:1	-101.9	0.401	2.28	0.176
	12:1	-104.6	0.482	2.43	0.198
14.0	15:1	-89.6	0.399	2.31	0.173
	12:1	-93.6	0.464	2.44	0.190

Table 4.3: Performance characteristics of model at suction pressure and compression ratio (60% R134a and 40% R23).

Suction Pressure (psia)	Compression Ratio	Evaporator Temperature (°F)	COP	Carnot COP	Second Law Efficiency (η_{II})
11.0	15:1	-106.6	0.453	2.28	0.199
	12:1	-109.0	0.527	2.44	0.216

Chapter 5

Experimental Procedures and Results

The analysis of the mixed refrigerant system model provides initial operation points in order to test the experimental system performance. The operating points are used to develop a procedure to examine compression ratio, separator performance, evaporating temperatures, refrigeration capacity and power consumption. In order to refine the design parameter under specific operating parameters, the mechanical components in the system will need to be adjusted as well as the chilled water/glycol used in the condensing separator.

5.1 Experimental Evaluation Devices

A data acquisition system is used to record the various system values for temperature, pressure, current and voltage measured at state points throughout the system. An instrumentation diagram for the mixed refrigerant system is presented in Figure 5.1. Type T thermocouples from Omega (Omega, 2012) are used to measure temperatures at the locations in Figure 5.1, labeled with a capital T followed by the location number. The thermocouples are fixed to the outer wall of the tubing throughout the system. Pressure transducers from Omega are used to measure the internal refrigerant pressures at the locations designated in Figure 5.1 with a capital P followed by the location number (Omega, 2012).

A Variac voltage regulator is used to change the voltage input and thus the power to the heater pads on the evaporator. Both voltage and current to the heater pads are measured and used to adjust the energy input to the evaporator. A Yokogawa power meter is used to measure the compressor power consumption (Yokogawa, 1998). Power consumption, current and voltage measurements are recorded through the data acquisition system and labeled on the instrumentation diagram in Figure 5.1.

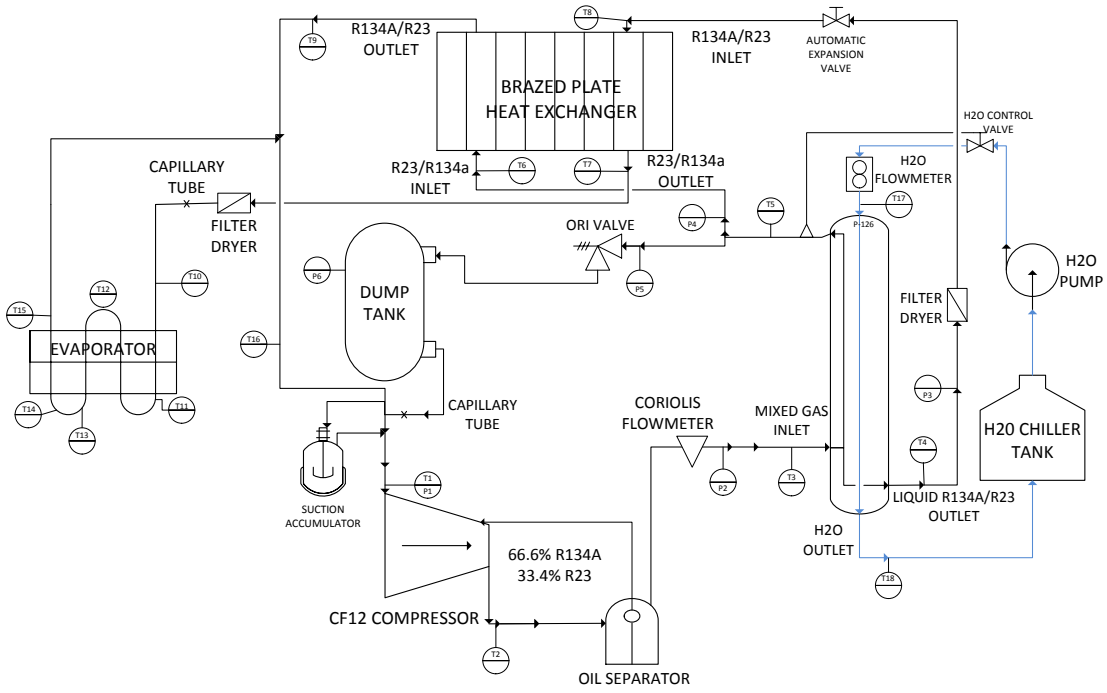

Figure 5.1: Instrumentation diagram for mixed refrigeration system schematic.

5.2 Prototype Apparatus

The mixed refrigerant system prototype apparatus described in section 4.2 is presented in further detail in this section. Component descriptions follow to provide physical illustrations of the refrigeration schematic in Figure 5.1. Figure 5.2 is an image of the entire mixed refrigeration system.

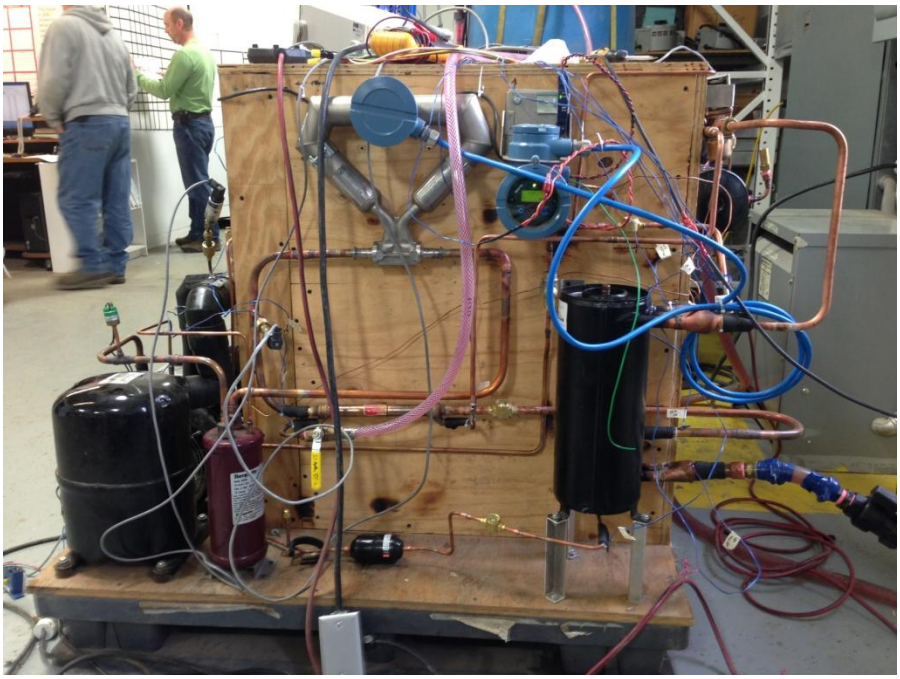

Figure 5.2: Mixed refrigerant system test apparatus.

A Copeland CF12 compressor (Emerson, 2010b) is a reciprocating compressor sized for this application and chosen because of its simple operation and well known performance. Due to the use of two refrigerants operating through the same compressor, a Temprite 903 (Temprite, 2009) oil separator is selected, which is oversized for the range of operating conditions of the mixed refrigerant apparatus.

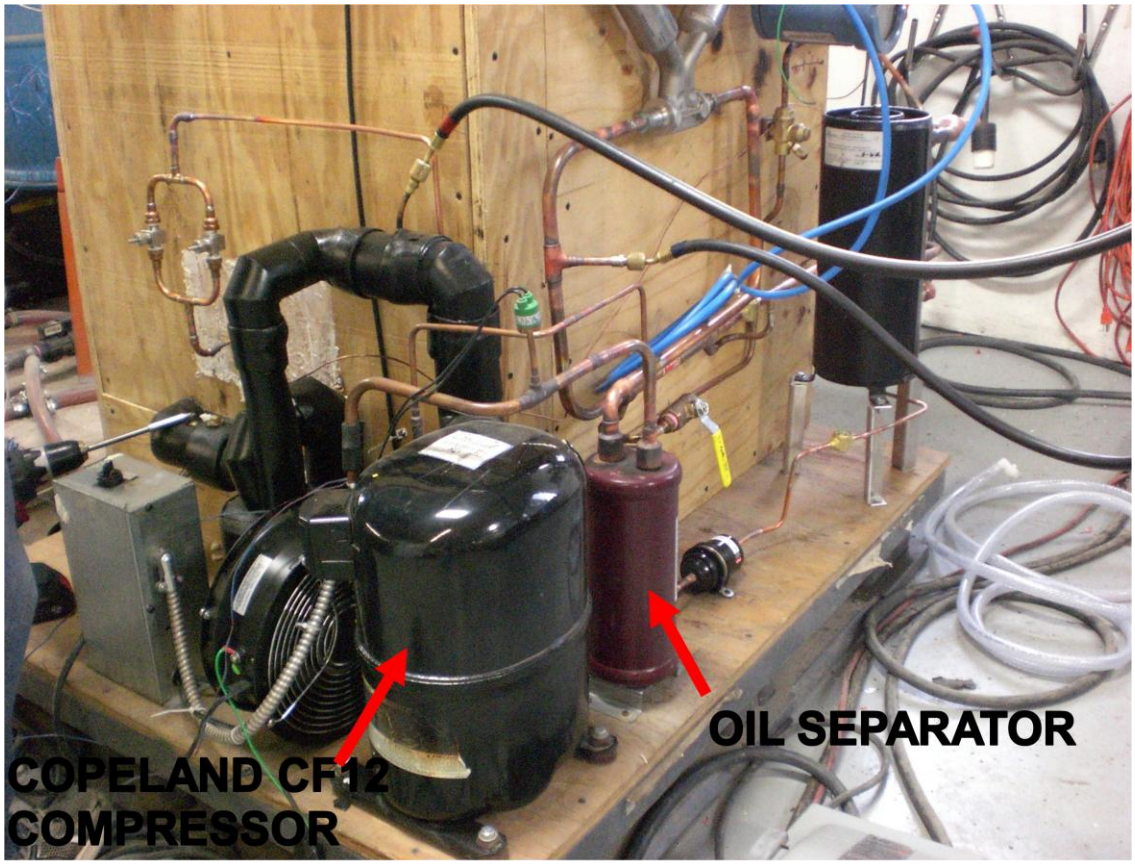

Figure 5.3: Copeland CF12 (Emerson, 2010b) compressor and Temprite (Temprite, 2009) oil separator.

A Micro Motion Coriolis (Emerson, 2011) flow meter is used at the outlet of the compressor, after the oil separator, to obtain an accurate measure of the mass flow rate of the mixed refrigerant flowing through the compressor, as shown in Figures 5.3 and 5.4. The refrigerant mixture then enters the condensing separator. A filter-dryer is placed at the outlet of the R134a-heavy liquid line leaving the bottom of the separator.

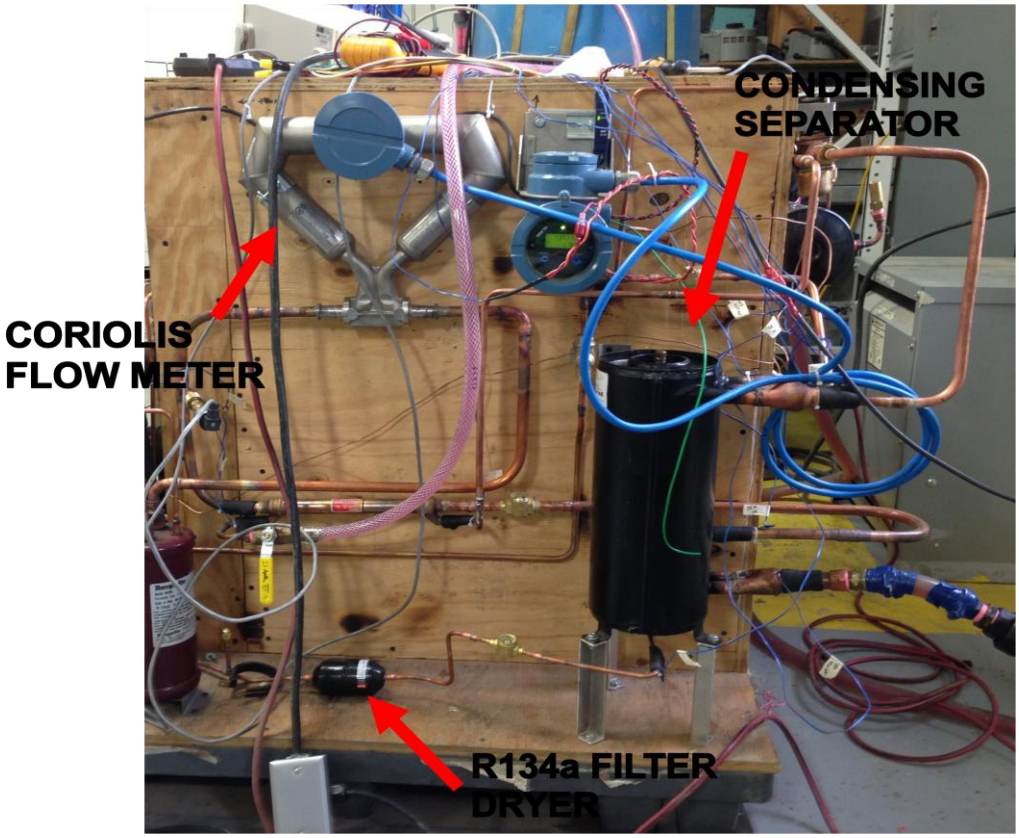

Figure 5.4: Coriolis flow meter (Emerson, 2011), condensing separator and R134a filter-dryer.

The heat exchanger used for the separator is an Aqua Systems coil in tube heat exchanger (Aqua Systems Inc., 2012), shown in detail in Figure 5.5. The refrigerant flows into the large cylinder and the water/glycol cooling fluid flows in a pipe that is coiled throughout the inside of the cylinder. The water/glycol pipe has fins to increase the heat transfer surface area on the condensing side of the heat exchanger. The R134a-heavy liquid mixture will leave through the bottom, and the R23-heavy vapor mixture will leave through the top of the cylinder. Refrigerant entering the separator flows into the side at the bottom third of the cylinder to allow for collection of the R134a-heavy liquid refrigerant mixture at the bottom of the cylinder. A sight glass is installed at the refrigerant mixture inlet and two outlets to monitor whether the flow is in a vapor mixture state.

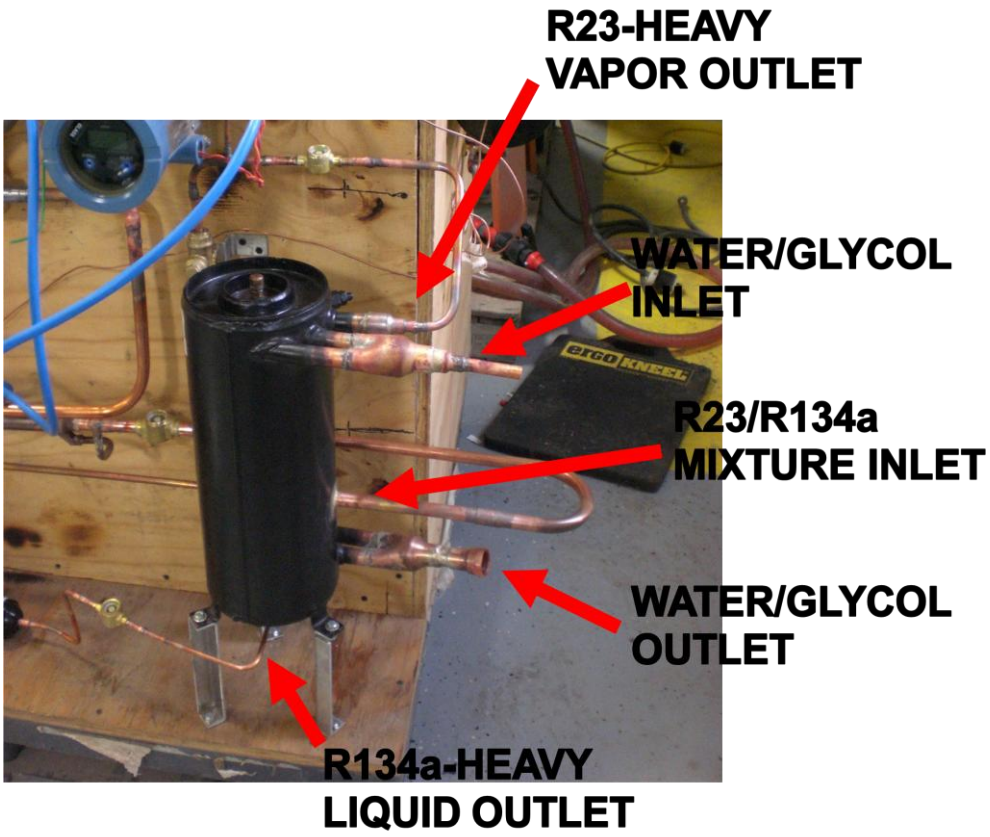

Figure 5.5: Condensing separator refrigerant and chiller connections.

An expansion tank is installed to allow for accumulation of the refrigerant if failure occurs or if the pressure in the system reaches an unsuitable level for the components. The expansion tank is shown in Figure 5.6 and consists of an open on rise of inlet (ORI) pressure valve and a refrigerant bleed valve line. The ORI valve is connected at the inlet of the expansion tank and is set to a desired pressure. If the refrigerant pressure in the system at the outlet of the compressor reaches the level at which the ORI valve is set then the valve opens and allows refrigerant to flow into the expansion tank. In the event that refrigerant enters the expansion tank, there is a small capillary tube connected to the expansion tank to allow for the refrigerant to bleed back into the suction side of the compressor.

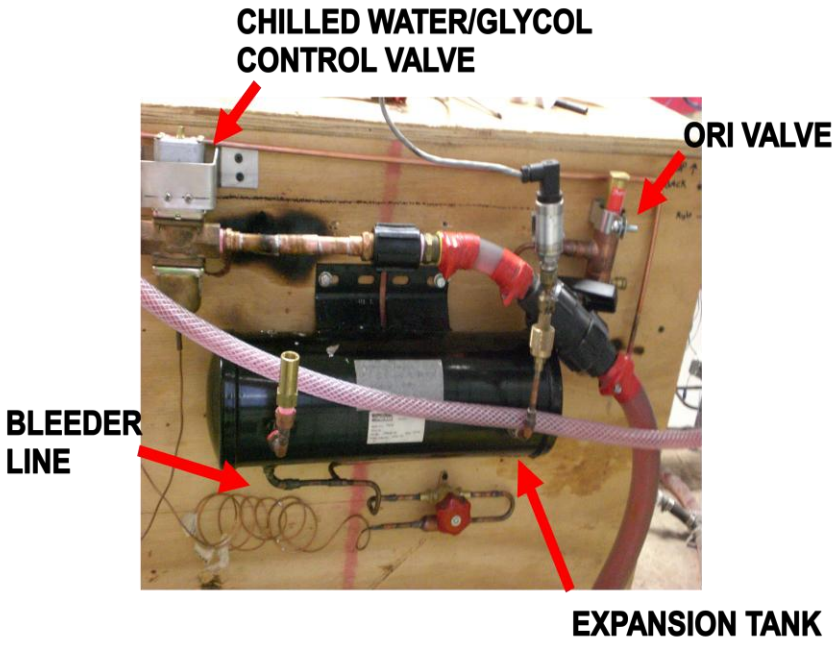

Figure 5.6: Mixed refrigerant system expansion tank.

The R134a-heavy refrigerant mixture leaves the separator in a liquid state and flows through a filter-dryer before entering the expansion valves. Two needle valves are used for the expansion valves to allow for the maximum adjustment while setting the suction pressure. The R134a-heavy refrigerant line that leaves the separator can be seen in Figure 5.5, while the expansion valves are shown in Figure 5.7.

A suction accumulator is installed before the inlet to the suction side of the compressor in the event that the refrigerant mixture leaving the evaporator and the brazed plate heat exchanger is in a liquid/vapor mixture state. The suction accumulator and the suction line of the compressor are shown in Figure 5.7. The R134a-heavy refrigerant mixture leaving the brazed plate heat exchanger and the R23-heavy refrigerant mixture leaving the evaporator both mix before exiting the insulated evaporator space. After both lines mix, the total refrigerant mixture flows through the suction accumulator where any remaining liquid refrigerant is trapped so that the refrigerant entering the suction side of the compressor is in a vapor state.

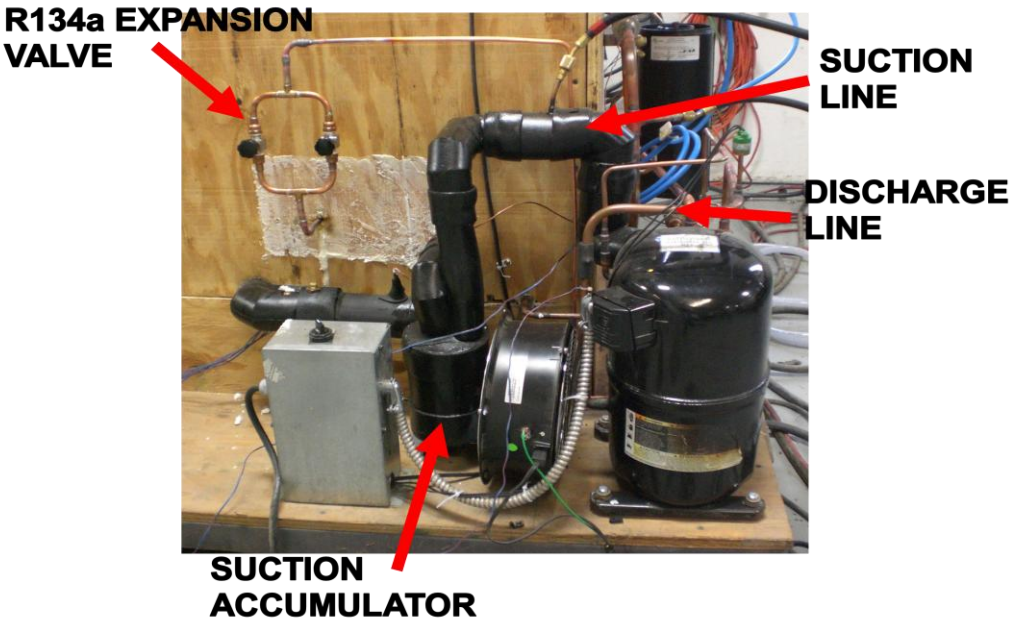

Figure 5.7: R134a expansion valves, suction accumulator and compressor suction line.

A counter-flow brazed plate heat exchanger is used for the inter-stage heat exchanger in which the R134a-heavy refrigerant mixture is used to condense the R23-heavy mixture. It is located behind the R134a expansion valves in Figure 5.7, covered by many layers of foam insulation. The counter-flow piping diagram for the two refrigerant mixtures is shown in Figure 5.8.

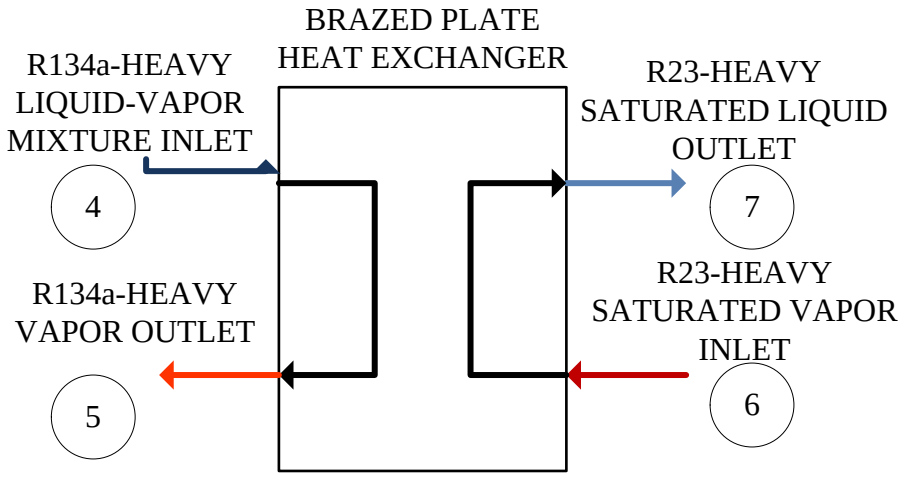

Figure 5.8: Brazed plate heat exchanger piping diagram.

The R23-heavy refrigerant mixture is condensed in the brazed plate heat exchanger and exits through a capillary tube. The capillary tube is 32 feet by 0.050 inches (JB 2004); was sized directly from the load and refrigerant requirements of a ULT freezer operating an evaporator at -87 °C (-124.6 °F). The entire length of the capillary tube is inside the insulated box and once the R23-heavy refrigerant mixture leaves the capillary tube it directly enters the evaporator. The evaporator consists of five plates with a combined length of 80 feet of copper tubing coiled inside the plates for the refrigerant. Air fills the volume of the plates that is not consumed by the refrigerant piping. This allows the system to cool a relatively small mass and reach steady state quicker than if a higher density liquid or solid was used in the evaporator plates. McMaster-Carr silicone heating pads (McMaster-Carr, 2012) are distributed evenly on the evaporator plates so that an even distribution of heat can be applied to the evaporator. The layout for the evaporator plates and the heating pads is shown in a diagram in Figure 5.9. The evaporator and heating pads are installed in an insulated box to maximize the energy entering the evaporator.

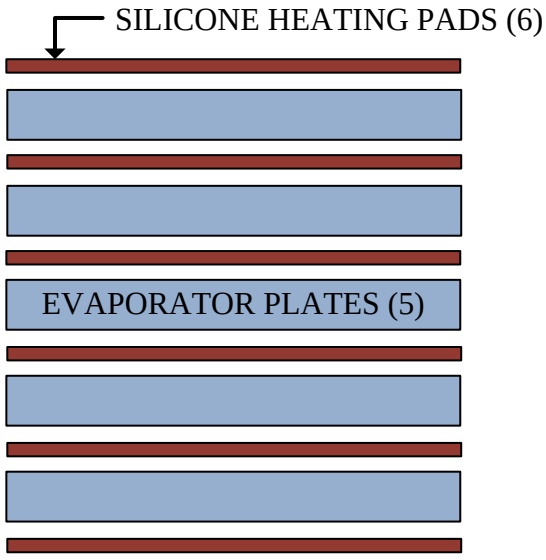

Figure 5.9: Side view of evaporator plates with heating pads.

5.3 Experimental Procedure

An experimental procedure is developed for each of the tests that is performed on the mixed refrigerant system. This is done to ensure that each test is carried out in the same manner as the one before to minimize the error that can come from varying the testing procedure. The chilled water/glycol system is adjusted to its desired set-point temperature, and then the refrigeration system is turned on. Once the refrigeration system is turned on, the suction pressure is set using the needle valve. Then, the discharge pressure is set using the temperature and flow rate of the chilled water/glycol system. After the operating parameters reach their desired operating point, the evaporator heat load is turned on. As long as the operating points are unchanged after the heat load is applied, then the mixed refrigeration system is allowed to run until it reaches a steady-state operating point.

The chilled water/glycol system is designed to be operated in a manner to ensure that the system components are not damaged; he pump is turned on, then the compressor for the chiller. Once the system power is on, the set-point temperature can be chosen. If the chiller system is being turned on for the first time, the chiller is allowed to run for approximately 20 minutes to give the system enough time to chill the water/glycol to the set-point temperature before a heat load is applied.

When the chiller system has cooled down the water/glycol mixture, the NetDaq data acquisition system is set up and a new file is started for the test. The mixed refrigeration system is turned on and the data acquisition system is checked to confirm the measurements are being recorded. A few minutes after the mixed refrigerant system is turned on, the needle valve is adjusted to set the suction pressure. This is done by reading the suction pressure from the data acquisition system until the desired suction pressure is obtained. After the suction pressure is set, the discharge pressure is set by adjusting the chilled water/glycol flow rate and the water/glycol temperature in the event that the chiller set-point temperature is too high or too low. This will

adjust the condensing pressure, and consequently the discharge pressure, as well as the condensing temperature inside the separator.

When both the suction pressure and discharge pressures are set to the appropriate values for the current test, the mixed refrigerant system is allowed to run and cool the evaporator plates. The system cools the plates until all of the evaporator thermocouples reach temperatures near the predicted low temperature from the refrigerant model analysis for the current test conditions.

Once the evaporator plates are cooled near the predicted temperature, the Variac is turned on to apply the desired heat load. This is done by measuring the voltage and current to determine the power input to the heater, in Watts. The heat load is adjusted to be slightly greater than the predicted heat load for the current test to ensure that the refrigerant mixture leaving the evaporator is a saturated vapor or slightly superheated. Adding more heat than the evaporator can remove will provide a slightly higher refrigeration capacity for the overall cycle, but ensure that the state point at the outlet of the evaporator can be defined.

The heat load will impact the suction and discharge pressures as the heat load settles throughout the system so adjustments are made to return the pressures to their original values. A test is complete once the mixed refrigerant system reaches a steady-state condition. The mixed refrigerant system has reached a steady-state condition when the thermocouples throughout the evaporator do not change more than ±1.5 °C for 20 minutes. After the completion of a desired test, new operational parameters are dialed in and the testing procedure commences again.

5.4 Experimental Results

Experimental results are monitored and recorded once the test reaches a steady-state condition according to the instrumentation diagram shown in Figure 5.1. Temperature and pressures are recorded following state points 1 through 9 as well as the additional points labeled in the instrumentation diagram. The mass flow rate is recorded for each test from the Micro Motion Coriolis (Emerson, 2011) flow meter (in lbm/hr). The heat load applied to the evaporator

is measured from the current and voltage to find the power in Watts and is calculated by the data acquisition system software. Results from the tests described in Chapter 4 are summarized in Table 5.1 for the suction and discharge pressure, mass flow rate, heat load and compressor power. Entire system results for tests 1 through 6 can be found in Appendix C.

Table 5.1: Results summary for experimental tests 1-6.

Test	Suction Pressure (psia)	Discharge Pressure (psia)	Mass Flow (lbm/hr)	Power (W)	Heat Load (W)
1	11.0	163.8	37.7	1152.9	302.7
2	11.5	131.7	48.4	1248.9	485.0
3	14.0	218.7	47.4	1306.7	400.5
4	14.2	172.2	82.4	1424.3	516.8
5	10.4	158.5	30.8	1046.0	334.4
6	11.2	134.6	45.5	1214.1	516.2

5.5 Experimental Performance Analysis

State point properties for the six tests in are presented in Tables C.7-C.12 in Appendix C. The overall system performance can be calculated using the coefficient of performance (COP) from Equation 4.18. The reversible Carnot COP is found from Equation 4.19 and the second law efficiency is found from Equation 4.20. The experimental performance results for tests one through four are presented in Table 5.2.

Table 5.2: Performance characteristics of model at suction pressure and compression ratio (66.6% R134a and 33.4% R23).

Suction Pressure (psia)	Compression Ratio	Evaporator Temperature (°F)	COP	Carnot COP	Second Law Efficiency (η_{II})
11.0	14.9:1	-103.0	0.263	2.36	0.111
11.5	11.4:1	-99.4	0.393	2.54	0.155
14.0	15.6:1	-81.4	0.310	2.47	0.125
14.2	12.1:1	-85.0	0.317	2.54	0.124

At a suction pressure of 11 psia, the COP, Carnot COP and Second Law Efficiency increase as the compression ratio decreases. This result is expected and is common to vapor compression refrigeration cycles. The evaporator temperatures recorded at each suction pressure are slightly different and this can be attributed to the slight difference in the recorded suction pressure and the difference in the mixture ratio of R134a to R23 in the evaporator for each case. For a suction pressure of 14 psia the COP and Carnot COP increase slightly as the compression ratio decreases. The Second Law Efficiency decreases slightly as the compression ratio decreases and does not follow the normal convention for a vapor compression refrigeration cycle. Figure 5.10 shows the second law efficiency as a function of the compression ratio for Tests 1-4.

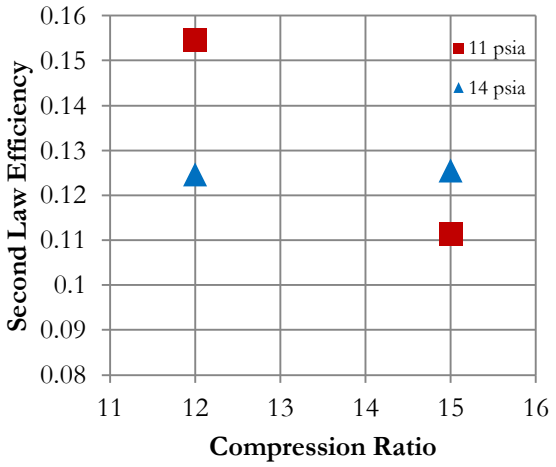

Figure 5.10: Second law efficiency at suction pressure for varying compression ratios.

The mass balance is analyzed at the condensing separator to determine the operating points that would provide better separation. Better separation is achieved when more of the R134a (and less of the R23) is condensed in the separator. It was found that the condensing temperature must be increased for the particular discharge pressure to improve the ratio of R134a to R23 in the saturated liquid line leaving the separator. This is a difficult phenomenon to achieve since the condensing temperature normally follows the saturation temperature at the discharge pressure for an azeotropic refrigerant. Since there is significant temperature glide (change in temperature from saturated vapor to saturated liquid states) in the condenser for the R134a-heavy mixture stream, it is hard to predict what the condensing temperature will be for a particular chilled water/glycol temperature and mass flow rate.

An alternative way to lower the evaporator temperature and increase the refrigeration capacity is to increase the amount of R23 in the vapor stream. It is found that the initial binary refrigerant ratio does not affect the saturated liquid mass fraction at a particular temperature and pressure. Therefore, increasing the amount of R23 in the initial binary refrigerant mixture ratio will increase the mass fraction of R23 in the vapor stream, but the R134a-heavy saturated liquid mass ratio will remain unchanged. The refrigerant mixture ratio is changed from 66.6% R134a and 33.4% R23 to a mixture of 60% R134a and 40% R23 by mass. Experimental tests are performed for the mixture at a suction pressure of 11 psia and compression ratios of 15:1 and 12:1. System results are presented in Table 5.1, while performance characteristics are in Table 5.3.

Table 5.3 lists the performance characteristics from tests five and six when the mixture ratio is changed to 60% R134a and 40% R23. The COP, Carnot COP and Second Law Efficiency with the adjusted initial refrigerant mixture show improved results from those with a mixture ratio of 66.6% R134a and 33.4% R23. Slightly lower evaporator temperatures are reached suggesting that the evaporator refrigerant mixture line contains more R23 than R134a. An increase in the

Second Law Efficiency from the first mixture ratio to the ratio with 60% R134a and 40% R23 shows an overall increase in the system performance at a suction pressure of 11 psia.

Table 5.3: Performance characteristics of model at suction pressure and compression ratio (60% R134a and 40% R23).

Suction Pressure (psia)	Compression Ratio	Evaporator Temperature (°F)	COP	Carnot COP	Second Law Efficiency (η_{II})
10.4	15.2:1	-109.8	0.32	1.96	0.16
11.2	12.0:1	-104.8	0.42	2.05	0.21

Chapter 6

Comparison of Mixed Refrigerant System Model and Experimental

The mixed refrigerant system model was developed to determine theoretical operating points and system performance at various initial conditions. Operating state points throughout the system at steady state are found to determine the lowest possible system temperature. Experimental procedures are developed to analyze the behavior of the mixed refrigerant system at at the same suction and discharge pressures. The overall system is evaluated on the basis of evaporating temperature, power consumption and the refrigeration capacity. Overall system performance is determined by the coefficient of performance (COP), reversible Carnot COP and the second law efficiency (η_{II}). Experimental results from tests one through four in are found in Table 5.2 in chapter 5 for the mixed refrigerant system with an overall mixture ratio of 66.6% R134a and 33.4% R23 by mass.

The evaporator temperatures predicted by the mixed refrigerant system model and the experimental results for tests one through four are presented in Table 6.1. Examination of the evaporator temperatures entering the evaporator shows that the experimental results are warmer than the theoretical model prediction at those conditions, except for the temperature recorded in Test 1. Outlet evaporator temperatures recorded in the experimental results were much warmer than calculated in the model. The evaporator temperatures measured are reasonably close to the predicted model temperatures because they are near the uncertainly range for the thermocouples of 1.8 °F. The modeled refrigerant evaporating temperatures are assumed to be the lowest temperature that the system could reach at those operating conditions. In Table 6.1 the error is calculated as the model temperature at the inlet or outlet minus the experimental temperature measured. For test 1 the error is positive, which suggests that there was not enough heat load applied to the evaporator to ensure that the R23-heavy stream was at least a saturated vapor.

Tests 2-4 have a negative error, therefore, the temperature leaving the evaporator is warmer than expected. This suggests that plenty of heat load was applied to tests 2-4 and the refrigerant mixture was in a saturated vapor or a superheated vapor state. Assuming that there is some inefficiency in the energy load entering the evaporator (that is not accounted for) and the mixture ratios calculated for the refrigerant streams are correct, the mixed refrigerant system is operating in reasonable agreement with the model prediction.

Table 6.1: Evaporator temperatures (°F) for model and experimental results (Tests 1-4).

Test		1	2	3	4
Inlet	Model	-101.9	-104.6	-89.0	-93.6
	Experiment	-103.0	-99.4	-81.4	-85.0
	Error	+1.1	-5.2	-7.6	-8.6
Outlet	Model	-58.7	-59.4	-48.8	-50.3
	Experiment	-71.6	-60.2	-12.1	-9.5
	Error	+12.9	+0.8	-36.7	-40.8

The model developed for the mixed refrigerant system uses an evaporator load that differs slightly from the actual applied load in the evaporator. The heat load applied for the experiments is greater than the predicted model load, to make sure the refrigerant mixture leaves the evaporator in a vaporous state. Heat load, along with compressor power, is presented for the model and experimental tests one through four in Table 6.2.

Table 6.2: Power consumption for model and experimental results (Tests 1-4).

Test		1	2	3	4
Heat Load (Btu/hr)	Model	875.0	1500.0	1400.0	1700.0
	Experiment	1032.7	1655.0	1355.4	1760.6
	Error	-157.7	-155.0	+44.6	-60.6
Power (Btu/hr)	Model	2181.9	3133.0	3505.5	3662.9
	Experiment	3933.0	4261.4	4458.6	4849.7
	Error	-1751.1	-1128.4	-953.1	-1186.8

The power calculated in the model is found assuming a suction pressure a temperature of 4.4 °C (40 °F) which is the temperature specified by Copeland for the suction inlet condition

(Emerson, 2010). The power is found in the model by assuming an isentropic efficiency of 50% because the compressor manufacturer does not provide performance data at such low suction pressures and evaporating temperatures for the binary refrigerant mixture. For the operating parameters in the mixed refrigerant system model, Table 6.2 shows that the power consumption predicted by the model using these assumptions is not an accurate representation of the actual power that will be measured, but provides an acceptable estimation for the initial calculations.

Performance of the overall mixed refrigerant system is determined by calculating COP, reversible Carnot COP and the second law efficiency. Performance results for the mixed refrigerant model and experimental tests one through four are presented in Table 6.3. The COP for the system is the actual performance that the mixed refrigerant system can achieve, while the Carnot COP is the theoretical maximum COP that could be reached if the system had no irreversibility. The second law efficiency is calculated to determine how well the system is performing relative to the theoretical maximum performance, measured by the Carnot COP.

Table 6.3: Performance characteristics of model and experimental system (Tests 1-4)

Test		COP	Carnot COP	Second Law Efficiency (η_{II})
1	Model	0.401	2.28	0.176
	Experiment	0.263	2.36	0.111
	Error	+0.138	-0.08	+0.065
2	Model	0.482	2.43	0.198
	Experiment	0.393	2.54	0.155
	Error	+0.089	-0.11	+0.043
3	Model	0.399	2.31	0.173
	Experiment	0.310	2.47	0.125
	Error	+0.089	-0.16	+0.048
4	Model	0.464	2.44	0.190
	Experiment	0.317	2.54	0.124
	Error	+0.147	-0.10	+0.066

Table 6.3 shows that the COP for the experimental tests are all slightly lower than the COP calculated from the mixed refrigerant model. The error is calculated by subtracting the

experimental value from the calculated model value. The error shows that the model predicts a higher COP and second law efficiency and a lower Carnot COP than is found in the experimental results. This illustrates that the mixed refrigerant system model does not predict the exact operation of the experimental system. For the most part, the model severely under predicts the power consumed by the compressor and could be improved by using a more accurate isentropic efficiency. The condensing temperature is assumed based on the temperature glide from saturated vapor to saturated liquid at the discharge pressure and the system model would improve greatly if the condensing temperature could be more accurately predicted.

It is expected that COP will increase as the compression ratio decreases; this is observed in both the model and the experimental data. For the conditions of test 4 (suction pressure of 14 psia and compression ratio of 12:1) the COP slightly increases from the values in Test 3 at a higher compression ratio. Under these operating conditions the COP and second law efficiency are lower than the same compression ratio in Test 2, but it was anticipated that Test 4 would produce more efficient results.

Table 6.4: Evaporator temperatures, power and heat load (Tests 5-6).

Test		5	6
Inlet Evap. (°F)	Model	-106.6	-109.0
	Experiment	-109.8	-104.8
	Error	+3.2	-4.2
Outlet Evap. (°F)	Model	-62.9	-64.2
	Experiment	-50.9	-32.2
	Error	-12.0	-32.0
Heat Load (Btu/hr)	Model	875.0	1500.0
	Experiment	1141.1	1761.3
	Error	-266.1	-261.3
Power (Btu/hr)	Model	1931.4	2847.0
	Experiment	3569.0	4142.6
	Error	-1637.6	-1295.6

Table 6.5: Performance characteristics of model and experimental system (Tests 5-6)

	Test	COP	Carnot COP	Second Law Efficiency (η_{II})
5	Model	0.453	2.28	0.199
	Experiment	0.319	1.96	0.163
	Error	+0.134	+0.32	+0.036
6	Model	0.527	2.44	0.216
	Experiment	0.425	2.56	0.166
	Error	+0.102	-0.12	+0.050

Experimental and model results for Tests 5-6 are presented in Table 6.4. The performance characteristics for the model show the expected performance that could be obtained by the experimental system. Measured performance for the experimental system in Table 6.5 shows that the system does not achieve the predicted model performance for the operating conditions. As the compression ratio decreases, the COP and second law efficiency increases. The experimental COP in Tests 5-6 (Table 6.5) show an increase from Tests 1-2 (Table 6.3) at the same suction and compression ratio conditions. An initial mass fraction of 60% R134a and 40% R23 provided the expected increase in overall system performance; this is due to the fact that the R23-heavy stream in the evaporator has an increased percentage of R23 compared with the initial mixture ratio of 66.6% R134a and 33.4% R23 by mass.

Chapter 7

Comparison of the Mixed Refrigerant and Cascade Systems

A model of the two-stage cascade refrigeration system was developed to determine the operating points of the refrigeration system. The cascade system is examined at three designed heat load and evaporator temperatures. The cascade unit that is tested was developed at Farrar Scientific in 2006 to reach typical ULT storage evaporator temperatures of -97 °C (-142.6 °F), -87 °C (-124.6 °F), and -82 °C (-115.6 °F). Experimental results are used to determine the overall performance of the system, measured by the evaporator temperature, heat load, power consumption, COP and second law efficiency. Table 7.1 shows that the evaporator temperature increased, the applied heat loads increased and the overall COP and second law efficiency for the cascade system increases.

Table 7.1: Performance characteristics of experimental cascade system (Tests 1c-3c)

Test	Evaporator Temperature (° F)	Heat Load (Btu/hr)	Power (Btu/hr)	COP	Carnot COP	Second Law Efficiency (η_{II})
1c	-142.6	1733.3	9598.6	0.18	1.47	0.163
2c	-124.6	3852.1	10643.9	0.36	1.62	0.22
3c	-115.6	5216.9	11594.2	0.45	1.74	0.26

The cascade refrigeration model predicted the operating conditions based on the suction pressure, discharge pressure and the heat load. The COP and second law efficiency follow the same trend predicted by the model and therefore, support the experimental results for the COP calculated based on measurements. Test number 3c, with an evaporator inlet temperature of -82 °C (-115.6 °F) and a refrigeration capacity of 1528.9 W (5216.9 Btu/hr), provides the closest operating point comparison to the performance of the mixed refrigerant system. Although the two-stage cascade refrigeration system uses R508B for the low-stage and R404A for the high-

stage, the system operates with the same Copeland CF series compressors and evaporator temperatures near those achieved in the mixed refrigerant system.

Comparing the mixed refrigerant system to the two-stage cascade system developed at Farrar Scientific provides the evaporator temperature, refrigeration capacity and performance that must be achieved for a mixed refrigerant system to become a viable option for replacing cascade systems in ULT refrigeration applications. For the two-stage cascade system, experimental results in Test 3c found an evaporator temperature of -82 °C (-115.6 ° F), refrigeration capacity of 1528.9 W (5216.9 Btu/hr), and overall COP of 0.45. The experimental results for the mixed refrigerant system closest to the cascade system were found in Test 5, when the mixed refrigerant system achieved an evaporator temperature of -78.8 °C (-109.8 °F), refrigeration capacity of 345.6 W (1179.1 Btu/hr) and a COP of 0.319. Although the refrigeration capacity of the mixed refrigerant system is lower than the two-stage cascade system, the power is significantly lower for the mixed refrigerant system at 3569.0 Btu/hr compared to 11,594.2 Btu/hr for the cascade system. However, the COP of the mixed refrigerant system is lower than the COP of the cascade cycle, indicating that the mixed refrigerant system would consume more power if both were sized to provide the same refrigeration capacity.

There are design features of the mixed refrigeration system that would need to be addressed to make the system viable for all applications. The high-stage condenser on the two-stage cascade system is an air-cooled heat exchanger, and the mixed refrigerant system has a water/glycol chilled condenser. It is common to use air-cooled condensers and the use of chilled water/glycol is expensive and requires another cooling system, which is not accounted for in the overall performance of the mixed refrigerant system.

The increased temperature glide throughout the evaporator in the mixed refrigerant system makes the system a less likely candidate for certain ULT applications since the temperature increase is significant. It would be difficult to predict what the actual temperature of the frozen samples would be held at due to the temperature glide. A design improvement could

be made at the evaporator to achieve a smaller temperature increase from the outlet of the expansion valve to the outlet of the evaporator. The refrigerant mixture at the end of the evaporator could be routed to an additional heat exchanger at the outlet of the brazed plate heat exchanger to subcool the R23-heavy stream.

Additional tests could be performed to determine the optimum R23 to R134a mixture ratio to achieve the best results for the current system configuration. As more R23 is added to the mixture, the brazed plate heat exchanger must be analyzed each time to ensure that the R134a-heavy stream can completely condense the R23-heavy stream. New refrigerant mixtures could be used in the current system configuration to produce improved results. Refrigerants such as R508B would be a good substitute for R23 since it is a mixture of R23 and R116.

Chapter 8

Conclusions & Recommendations

A model was developed for a mixed refrigerant system model designed to reach ultra-low temperatures (ULT) and provide refrigeration capacities typical for refrigeration storage. Using the model, operating conditions were predicted for a prototype experimental mixed refrigerant system. The model was used to predict the heat load to be applied during experimental testing and to analyze the experiments results to determine overall system coefficient of performance (COP), Carnot COP, and second law efficiency. The mixed refrigerant system performance was compared to a two-stage cascade refrigeration system designed for similar ULT refrigeration storage applications. The model and experimental results of the mixed refrigerant system were used to provide design recommendations for system improvements and operating condition specifications.

The overall system COPs calculated for the mixed refrigerant system were lower than those of the cascade system and the evaporator temperatures were slightly higher. The highest overall COP achieved in the mixed refrigerant system was 0.425, found in Test 6 with a mixture ratio of 60% R134a and 40% R23, suction pressure of 11 psia and compression ratio of 12:1. This was close to the COP of 0.45 found in Test 3c for the cascade system. However, the single compressor in the mixed refrigerant system did not produce as high of a refrigeration capacity as the cascade system, but shows promise to achieve similar COPs.

The evaporating temperature in the system was sensitive to the expansion valve set point, so the temperature in the mixed refrigerant system could reach that of Test 3c for the cascade system. While the overall system performance of the mixed refrigerant system was in the range for a normal two-stage cascade refrigeration system, the significant temperature glide in the evaporator made the sample storage temperature much warmer than the cascade system. Physical

system design improvements could alleviate this problem by subcooling the R23-heavy stream with the outlet line of the evaporator. This would increase the refrigeration capacity at those conditions and provide a lower temperature R23-heavy stream leaving the evaporator.

Overall system performance of the mixed refrigerant system as measured by the COP and second law efficiency showed that the mixed refrigerant system could be implemented for ULT applications. The model for the mixed refrigerant system predicted trends that were confirmed by the experimental testing, although the error in the model results shows room for improvement in the model design. Although the mixture ratios calculated for the mixed refrigerant system were assumed to be the same throughout the system; experimental results were similar to predicted. Measuring the actual refrigerant mixture ratios at different points in the system would provide a more accurate measure of system performance. Increasing the amount of R23 in the overall mixture ratio showed improved system performance and suggests a path to further enhancement. Further experimental testing with mixture ratios leaving more R23 in the vapor stream at the separator exit will provide an alternative design for ULT refrigeration.

BIBLIOGRAPHY

ASHRAE. (2010). ASHRAE Handbook-Refrigeration. Atlanta, GA: American Society of Heating, Refrigeration and Air-Conditioning, Inc.

Aqua Systems Inc. (2012). Aqua Systems Heat Exchanger Models: S-6. Retrieved from http://www.aquasystemsinc.com/models_test.html

Cengel, Y.A., and Boles, M.A.. (2010). Thermodynamics: An Engineering Approach (7th ed.). New York, NY: McGraw-Hill.

Chen, J.X., Hu, P., & Chen, Z.S.. (2008). Study on the Ineration Coefficients in PR Equation with vdW Mixing Rules for HFC and HC Binary Mixtures. International Journal of Thermophysics, 29, 1945-1953.

Dalkilic, A.S., & Wongwises, S.. (2010). A Performance Comparison of Vapor-Compression Refrigeration System Using Various Alternative Refrigerants. International Communications in Heat and Mass Transfer, 37: 1340-1340.

Dincer, Ibrahim. (2003). Refrigeration Systems and Applications. West Sussex, England: John Wiley & Sons, Ltd.

DuPont. (2005). Thermodynamic Properties of DuPont Suva 404A (HP62) Refrigerant. Available from DuPont Online Database.

DuPont. (2004). Thermodynamic Properties of DuPont HFC-134a (134a Refrigerant). Available from DuPont Online Database.

DuPont. (2004). Thermodynamic Properties of DuPont Suva 95 Refrigerant (R-508B). Available from DuPont Online Database.

DuPont. (1994). Thermodynamic Properties of DuPont HFC-23 (Freon 23). Available from DuPont Online Database.

Emerson Climate Technologies, Inc. (2010a). Copeland CF09K6E-TF5. Available from Emerson Climate Technologies Inc. customer database.

Emerson Climate Technologies, Inc. (2010b). Copeland CF12K6E-PFV. Available from Emerson Climate Technologies Inc. customer database.

Emerson Climate Technologies, Inc. (2011). Micro Motion Elite CMF050. Available from Emerson Climate Technologies Inc. customer database.

F-Chart Software. (2011). Engineering Equation Solver, Version 8.889.

Gong, M., Sun, Z., Wu, J., Zhang, Y., Meng, C., & Zhou, Y.. (2009). Performance of R170 Mixtures as Refrigerants for Refrigeration at -80 °C Temperature Range. International Journal of Refrigeration, 32, 892-900.

JB. (2004). Application and Engineering Data: Copper Capillary Tubing. Retrieved from http://www.jbind.com/products/product-search-results.aspx?category=capillary_tubing

Kim, S.G., & Kim, M.S.. (2002). Experiment and simulation on the performance of an autocascade refrigeration system using carbon dioxide as a refrigerant. International Journal of Refrigeration, 25, 1093-1101.

McMaster-Carr. (2012). McMaster-Carr: Flexible Silicone-Rubber Heat Sheets. Retrieved from http://www.mcmaster.com/#heat-blankets/=m0wqdp

Mehrabian, M.A., and Samadi, B.. (2010). Heat-transfer characteristics of wet heat exchangers in parallel-flow and counter-flow arrangements. International Journal of Low-Carbon Technologies, 5: 256-263.

Missimer, D.J.. (1997). Refrigerant Conversion of Auto-Refrigerating Cascade (ARC) Systems. International Journal of Refrigeration, 20: 201-207.

NIST Standard Reference Database 23. (2007). NIST Thermodynamics and Transport Properties of Refrigerants and Refrigerant Mixtures, REFPROP, Version 8.0.

Omega. (2012). Type T Thermocouple: Revised Type T Reference Tables. Retrieved from http://www.omega.com/prodinfo/thermocouples.html

Parekh, A.D., Tailor, P.R., and Jivanramajiwala, H.R.. (2010). Optimization of R507A-R23 Cascade Refrigeration System using Genetic Algorithm. World Academy of Science, Engineering and Technology, 70: 4-8.

Temprite. (2009). Temprite Product Catalog: 900 Series. Retrieved from http://www.temprite.com/main_content.asp?pagename=resources

Wallace, Roslyn. (1964). Studies on preservation by freezing of human diploid cell strains. Proceddings of the Society for Experimental Biology and Medicine, 116, 990-998.

Wang, Q., Cui, K., Sun, T., & Chen, G.. (2011). Performance of a single-stage auto-cascade operating with a rectifying column at the temperature level of -60°C. Applied Physics and Engineering, 12, 130-145.

Yokogawa. (1998). WT110/WT130 Digital Power Meter: User's Manual. Newman, GA.

Appendix A: Two-Stage Cascade System Results

Table A.1: Evaporator capacity of 1733 Btu/hr and suction pressure of 8.0 psia.

Low-Stage (R508B)

States	P (psia)	T (° F)	h (Btu/lbm)	s (Btu/lbm-R)
5	8.0	-143.5	-2.1	0.00602
6’	8.0	-142.3	45.9	0.1578
6	8.0	40	74.4	0.2281
7’	107	210.7	105.4	0.2281
7	107	351.8	136.4	0.2700
8	107	-47.2	-2.1	-0.00505

High-Stage (R404A)

States	P (psia)	T (° F)	h (Btu/lbm)	s (Btu/lbm-R)
1	15.0	-50.4	0.4038	0.001126
2’	15.0	-49.1	83.2	0.231
2	15.0	40.0	100.5	0.2412
3’	195.0	193.0	128.6	0.2412
3	195.0	299.5	156.5	0.2807
4	195.0	-39.2	0.4038	0.08264

Table A.2: Evaporator capacity of 3852 Btu/hr and suction pressure of 14.0 psia.

Low-Stage (R508B)

States	P (psia)	T (° F)	h (Btu/lbm)	s (Btu/lbm-R)
5	14.0	-127.1	1.5	0.01327
6’	14.0	-126.4	47.6	0.1519
6	14.0	40.0	74.2	0.2162
7’	136.0	190.5	100.7	0.2162
7	136.0	312.6	127.2	0.2535
8	136.0	-35.0	1.5	0.00347

High-Stage (R404A)

States	P (psia)	T (° F)	h (Btu/lbm)	s (Btu/lbm-R)
1	19.0	-40.6	43.6	0.1044
2’	19.0	-40.0	84.5	0.2017
2	19.0	40.0	100.3	0.2361
3’	223.0	189.7	126.8	0.2361
3	223.0	289.8	153.3	0.2740
4	223.0	91.2	43.6	0.0890

Table A.3: Evaporator capacity of 5217 Btu/hr and suction pressure of 17.0 psia.

Low-Stage (R508B)

States	P (psia)	T (° F)	h (Btu/lbm)	s (Btu/lbm-R)
5	17.0	-121.0	3.6	0.01822
6’	17.0	-120.3	48.3	0.1500
6	17.0	40.0	74.1	0.2121
7’	155.0	187.1	99.7	0.2121
7	155.0	305.0	125.3	0.2483
8	155.0	-28.0	3.6	0.00835

High-Stage (R404A)

States	P (psia)	T (° F)	h (Btu/lbm)	s (Btu/lbm-R)
1	22.0	-34.7	44.5	0.1049
2’	22.0	-34.1	85.3	0.2008
2	22.0	40.0	100.1	0.2328
3’	230.0	183.0	125.1	0.2328
3	230.0	278.4	150.1	0.2691
4	230.0	93.5	44.5	0.0905

Appendix B: Mixed Refrigerant System Model Results

For a suction pressure of 75.8 kPa (11 psia) and a compression ratio of 15:1, the state points for the mixed refrigerant system are shown in Table B.1. The mixed refrigeration system is also analyzed with a compression ratio is of 12:1 to determine the performance benefits of lowering the condensing pressure at the same suction pressure. The results for these operating conditions are presented in Table B.2.

Table B.1: Suction pressure of 11 psia and compression ratio of 15:1 (66.6% R134a|33.4% R23).

States	P (psia)	T (°F)	h (Btu/lbm)	s (Btu/lbm-R)
1	11.0	40.0	109.0	0.2728
2’	165	226.5	143.6	0.2728
2	165	366.8	178.2	0.3186
3	165	55.5	31.0	0.0657
4	11.0	-52.1	31.0	0.0798
5	11.0	-36.7	96.0	0.2357
6	165.0	55.5	103.1	0.2133
7	165.0	9.6	15.9	0.0353
8	11.0	-101.9	15.9	0.0506
9	11.0	-58.7	90.5	0.2466

Table B.2: Suction pressure of 11 psia and compression ratio of 12:1 (66.6% R134a|33.4% R23).

States	P (psia)	T (°F)	h (Btu/lbm)	s (Btu/lbm-R)
1	11.0	40.0	109.0	0.2728
2’	132.0	209.4	140.5	0.2728
2	132.0	340.4	172.0	0.2728
3	132.0	41.9	25.9	0.0557
4	11.0	-53.3	25.9	0.0667
5	11.0	-36.0	96.2	0.2352
6	132.0	41.9	101.8	0.2157
7	132.0	-4.6	11.2	0.0254
8	11.0	-104.6	11.2	0.0375
9	11.0	-59.4	90.4	0.2469

The mixed refrigerant system is also modeled at a suction pressure of 96.5 kPa (14 psia) for both compression ratios of 15:1 and 12:1 to develop a system trend for performance at various suction pressures. Tables B.3 and B.4 show the operating points of the mixed refrigerant system model at a suction pressure of 14 psia for compression ratios of 15:1 and 12:1, respectively.

Table B.3: Suction pressure of 14 psia and compression ratio of 15:1 (66.6% R134a|33.4% R23).

States	P (psia)	T (°F)	h (Btu/lbm)	s (Btu/lbm-R)
1	14.0	40.0	108.9	0.2672
2’	210.0	229.3	143.2	0.2672
2	210.0	366.7	177.5	0.3125
3	210.0	71.9	36.2	0.7546
4	14.0	-42.9	36.2	0.0906
5	14.0	-28.4	97.2	0.2338
6	210.0	71.9	104.5	0.2102
7	210.0	27.9	22.0	0.0479
8	14.0	-89.0	22.0	0.0645
9	14.0	-48.8	92.0	0.2427

Table B.4: Suction pressure of 14 psia and compression ratio of 12:1 (66.6% R134a|33.4% R23).

States	P (psia)	T (°F)	h (Btu/lbm)	s (Btu/lbm-R)
1	14.0	40.0	108.9	0.2672
2’	168.0	211.7	140.1	0.2672
2	168.0	339.9	171.3	0.3097
3	168.0	57.0	31.1	0.0658
4	14.0	-44.4	31.1	0.0780
5	14.0	-27.8	97.4	0.2335
6	168.0	57.0	103.3	0.2129
7	168.0	11.5	16.5	0.0366
8	14.0	-93.6	16.5	0.03277
9	14.0	-50.3	91.7	0.2432

Tests 5 and 6 are presented in Table B.5 and B.6 with an initial mixture ratio of 60% R134a and 40% R23. Tables B.5 and B.6 show the operating points of the mixed refrigerant system model at a suction pressure of 75.8 kPa (11 psia) for compression ratios of 15:1 and 12:1, respectively.

Table B.5: Suction pressure of 11 psia and compression ratio of 15:1 (60% R134a|40% R23).

States	P (psia)	T (°F)	h (Btu/lbm)	S (Btu/lbm-R)
1	11.0	40.0	108.5	0.2762
2’	165.0	232.5	144.4	0.2762
2	165.0	375.0	180.3	0.3211
3	165.0	48.4	28.1	0.0601
4	11.0	-57.8	28.1	0.0741
5	11.0	-38.5	95.5	0.2368
6	165.0	48.4	101.4	0.2121
7	165.0	5.4	14.6	0.0326
8	11.0	-106.6	14.6	0.0478
9	11.0	-62.9	89.6	0.2481

Table B.6: Suction pressure of 11 psia and compression ratio of 12:1 (60% R134a|40% R23).

States	P (psia)	T (°F)	h (Btu/lbm)	s (Btu/lbm-R)
1	11.0	40.0	108.5	0.2762
2’	132.0	214.9	141.0	0.2762
2	132.0	346.3	173.5	0.3177
3	132.0	34.8	23.6	0.0513
4	11.0	-59.5	23.6	0.0625
5	11.0	-38.0	95.6	0.2364
6	132.0	34.8	100.2	0.2149
7	132.0	-9.0	9.9	0.0224
8	11.0	-109.0	9.9	0.0346
9	11.0	-64.2	89.3	0.2485

Appendix C: Mixed Refrigerant System Experimental Results

The first test that the mixed refrigeration system is analyzed at is a suction pressure of 11 psia and a compression ratio of 15:1. The system pressures for test 1 are presented in Figure C.1 and temperatures recorded in the evaporator are presented in Figure C.2.

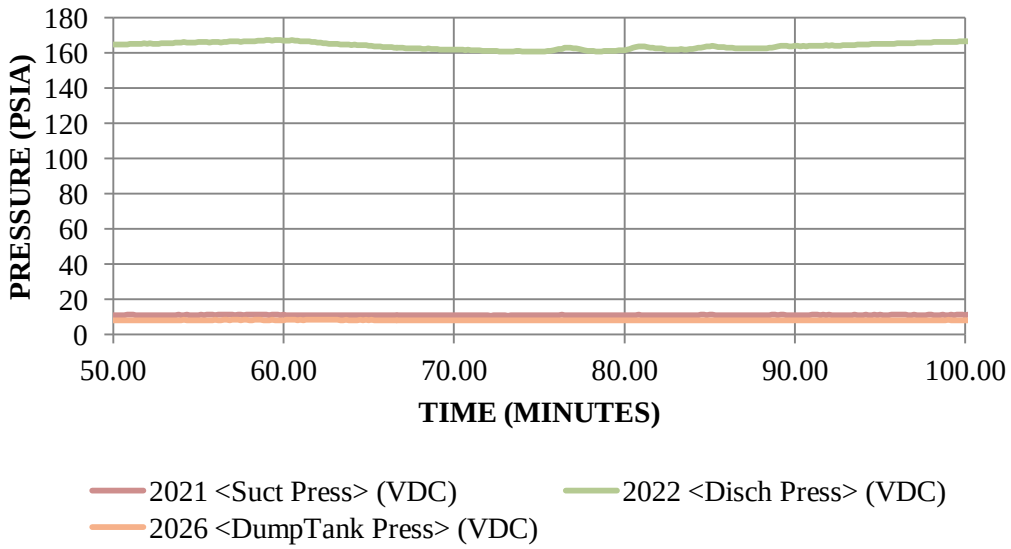

Figure C.1: Test 1 system pressures for suction pressure of 11 psia and CR of 15:1.

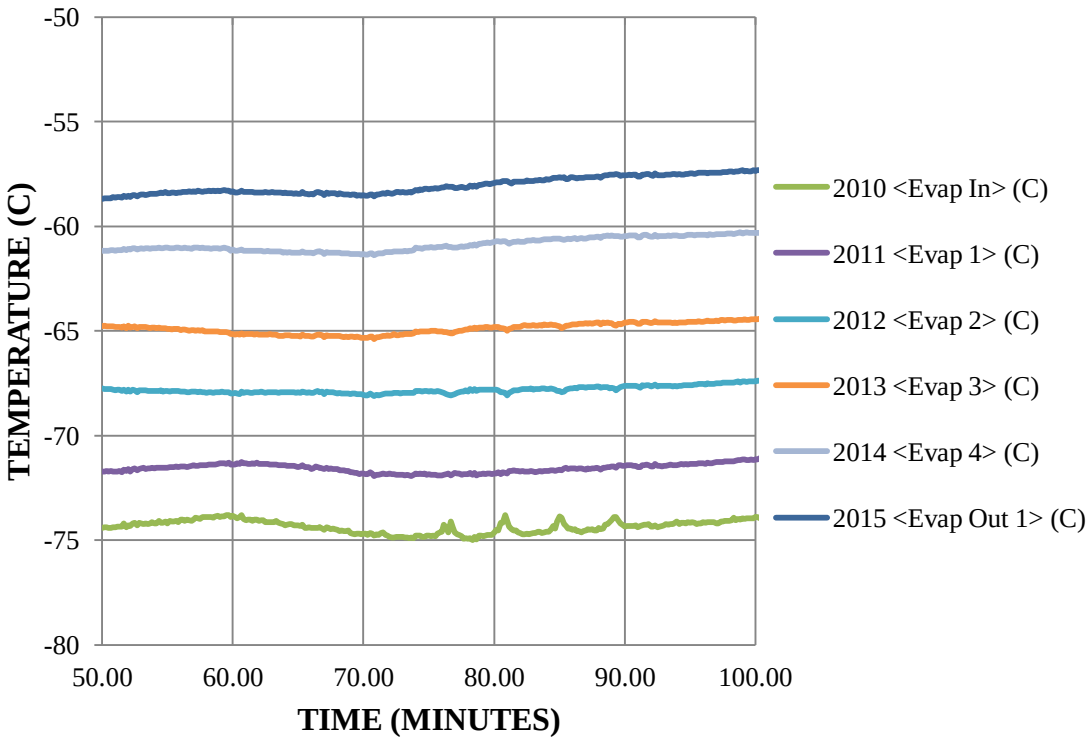

Figure C.2: Test 1 temperatures recorded at evaporator plates.

The measurements recorded for the temperature, pressure, mass flow rate, heat load and compressor power consumption for a suction pressure of 11 psia and a compression ratio of 15:1 is presented in Table C.1.

Table C.1: Experimental results for Test 1 at 11 psia suction pressure and 15:1 compression ratio.		
Mass flow rate (lbm/hr)	37.7	
Power (Watts)	1152.9	
Heat Load (Watts)	302.7	
State Point	Temperature (°C)	Pressure (psia)
1	-21.0	11.0
2	100.2	163.8
3	22.0	163.8
4	10.9	163.8
5	9.8	163.8
6	12.8	163.8
7	-19.9	163.8
8	-45.8	11.0
9	12.0	11.0
10	-74.3	11.0
11	-71.4	11.0
12	-67.6	11.0
13	-64.6	11.0
14	-60.4	11.0
15	-57.5	11.0
16	-44.7	11.0
17	8.8	N/A
18	8.9	N/A

The second test for the mixed refrigerant system is analyzed at a suction pressure of 11 psia and the compression ratio is changed from 15:1 to 12:1. Therefore, the discharge pressure is set to 132 psia. The system pressures and the temperatures recorded throughout the evaporator are presented in Figures C.3 and C.4. Table C.2 shows the measurements recorded for test number two.

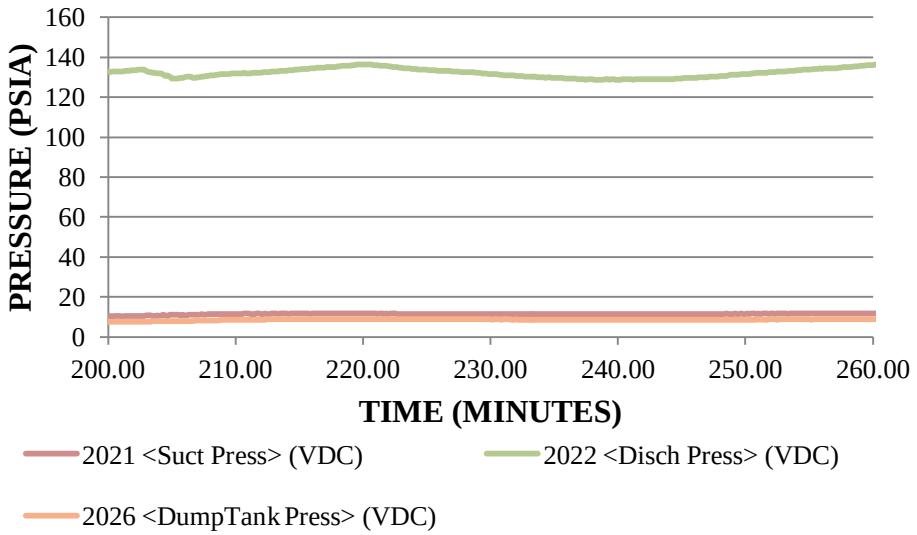

Figure C.3: Test 2 system pressures for suction pressure of 11 psia and CR of 12:1.

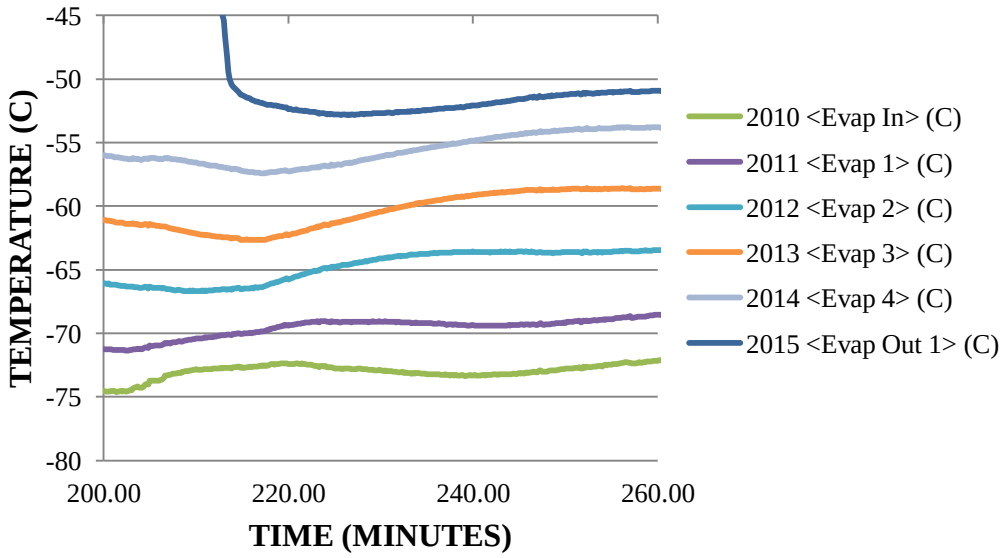

Figure C.4: Test 2 temperatures recorded throughout evaporator.

Table C.2: Experimental results for Test 2 at 11 psia suction pressure and 12:1 compression ratio.		
Mass flow rate (lbm/hr)	48.4	
Power (Watts)	1248.9	
Heat Load (Watts)	485.0	
State Point	Temperature (°C)	Pressure (psia)
1	-7.2	11.5
2	103.5	131.7
3	21.4	131.7
4	7.2	131.7
5	6.6	131.7
6	10.1	131.7
7	-30.6	131.7
8	-43.4	11.5
9	8.3	11.5
10	-72.7	11.5
11	-69.1	11.5
12	-63.6	11.5
13	-58.6	11.5
14	-54.0	11.5
15	-51.2	11.5
16	-14.8	11.5
17	5.7	N/A
18	5.7	N/A

The third test that the mixed refrigerant system is examined at is one where the suction pressure is set to 14 psia and a compression ratio of 15:1. A test similar to test number two is examined for test four when the suction pressure is set to 14 psia and the compression ratio is changed from 15:1 to 12:1. The recorded system pressures are presented in Figure C.5 and C.7, respectively. Also, temperatures recorded in the evaporator are presented in Figures C.6 and C.7

for tests three and four, respectively. Also the system measurements for test three and four are presented in Tables C.3 and C.4.

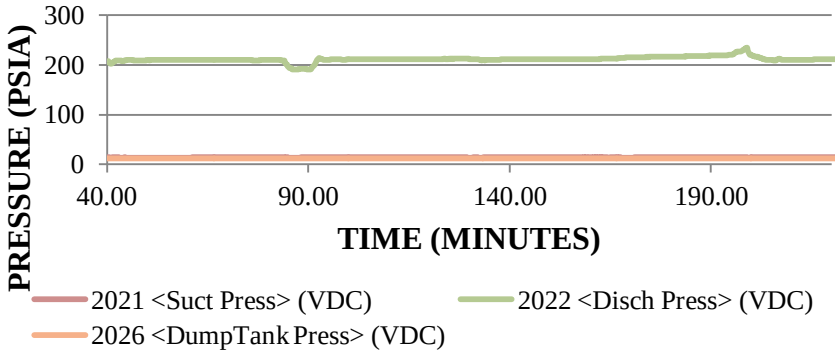

Figure C.5: Test 3 system pressures for suction pressure of 14 psia and CR of 15:1.

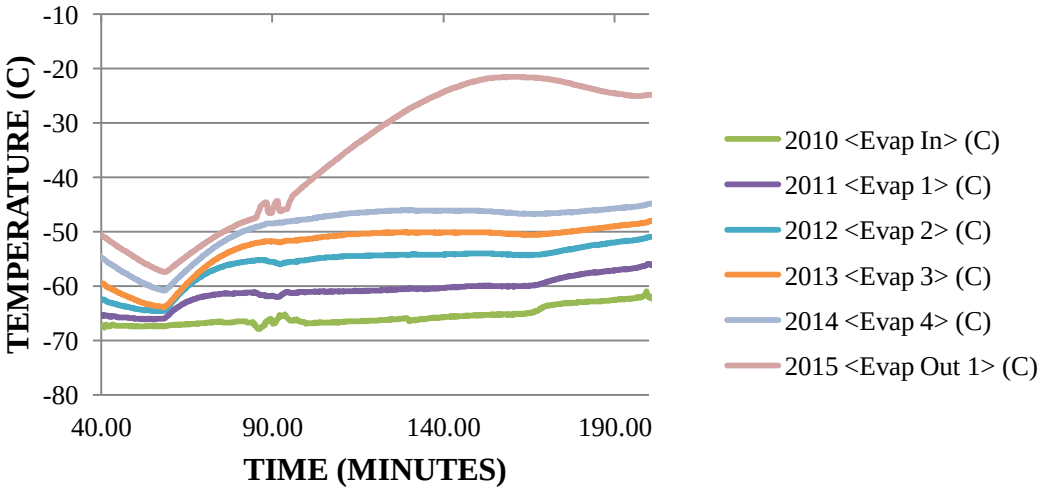

Figure C.6: Test 3 temperatures recorded in the evaporator.

Table C.3: Experimental results for Test 3 at 14 psia suction pressure and 15:1 compression ratio.		
Mass flow rate (lbm/hr)	47.4	
Power (Watts)	1306.7	
Heat Load (Watts)	400.4	
State Point	Temperature (°C)	Pressure (psia)
1	8.7	14.0
2	111.4	218.7
3	22.	218.7
4	22.7	218.7
5	23.1	218.7
6	22.7	218.7
7	-4.9	218.7
8	-38.5	14.0
9	22.7	14.0
10	-62.6	14.0
11	-57.1	14.0
12	-52.0	14.0
13	-49.0	14.0
14	-45.7	14.0
15	-24.5	14.0
16	2.7	14.0
17	23.2	N/A
18	24.1	N/A

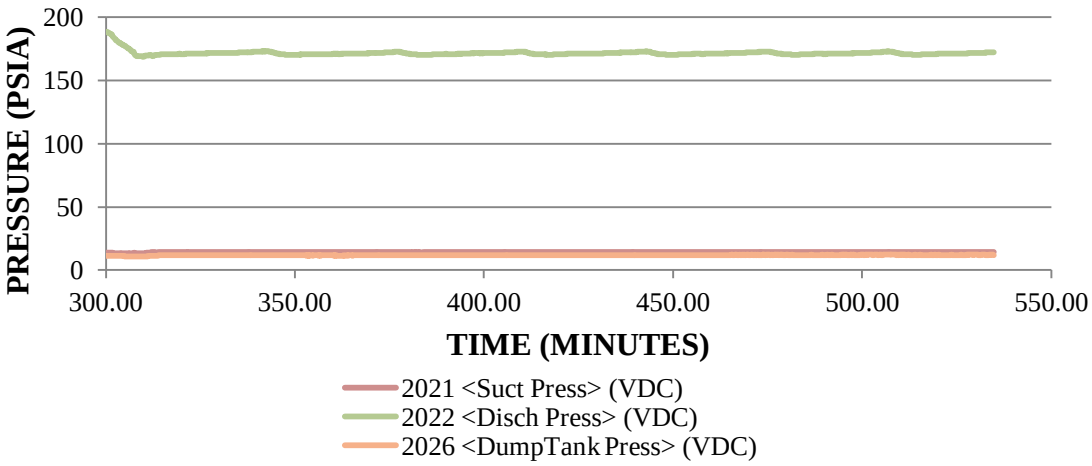

Figure C.7: Test 4 system pressures at suction pressure of 14 psia and CR of 12:1.

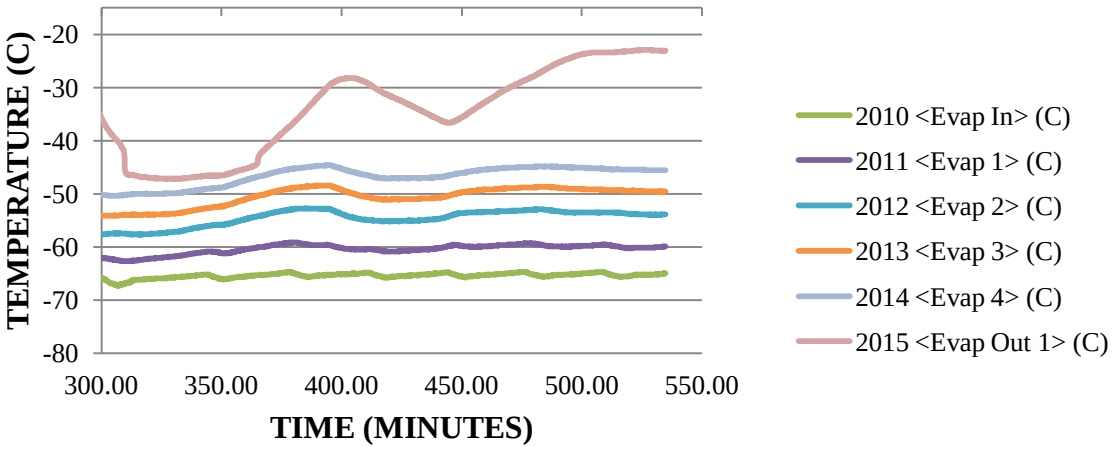

Figure C.8: Test 4 temperatures measured in the evaporator.

Table C.4: Experimental results for Test 4 at 14 psia suction pressure and 12:1 compression ratio.		
Mass flow rate (lbm/hr)	82.4	
Power (Watts)	1424.3	
Heat Load (Watts)	516.8	
State Point	Temperature (°C)	Pressure (psia)
1	6.3	14.2
2	110.1	172.2
3	24.1	172.2
4	22.7	172.2
5	16.2	172.2
6	17.4	172.2
7	-16.4	172.2
8	-36.2	14.2
9	16.2	14.2
10	-64.9	14.2
11	-59.8	14.2
12	-53.8	14.2
13	-49.5	14.2
14	-45.5	14.2
15	-23.0	14.2
16	2.5	14.2
17	15.7	N/A
18	17.1	N/A

From the analysis of the mixed refrigerant system at the operating points discussed above, the model of the refrigerant cycle showed that the performance of the system could be improved by altering the initial refrigerant mixture. For the fifth test the mixed refrigerant system is analyzed with an initial refrigerant mixture of 40% R23 and 60% R134a by mass. To determine how the system operates with the new mixture ratio. test number five examines the system at a suction pressure of 11 psia and a compression ratio of 15:1. Figure C.9 shows the

system pressures and temperatures measured in the evaporator are presented in Figure C.10. Recorded measurements for test five are found in Table C.5.

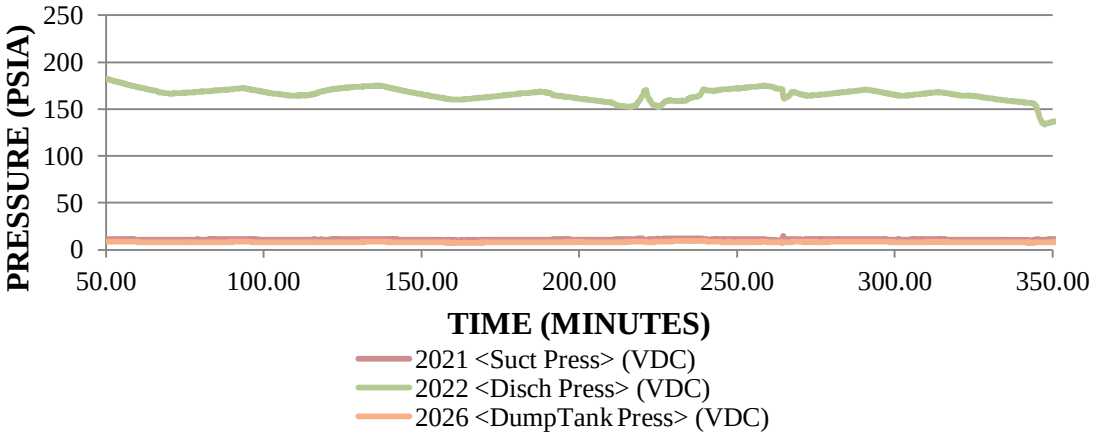

Figure C.9: Test 5 system pressures for mixture ratio of 40% R23 and 60% R134a.

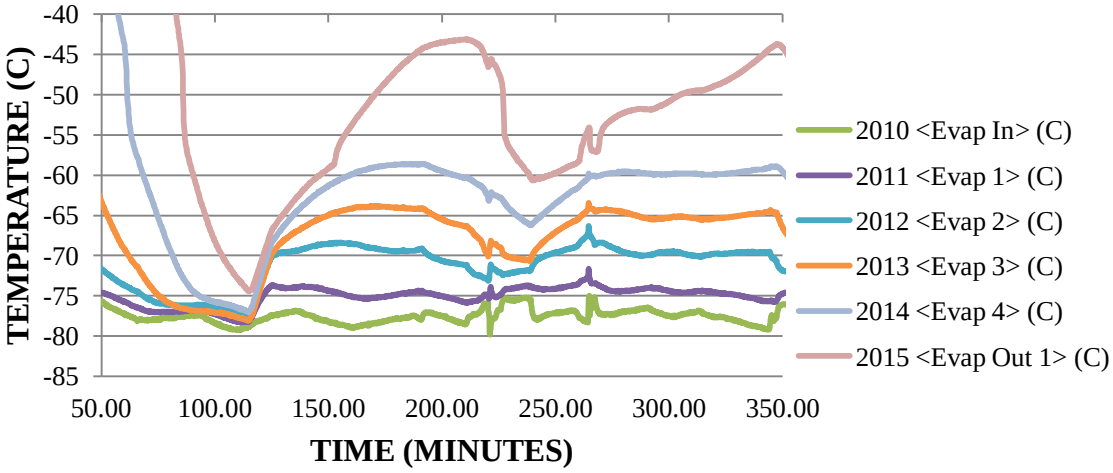

Figure C.10: Test 5 temperatures recorded in the evaporator.

Table C.5: Test 5 results with mixture ratio of 40% R23 and 60% R134a.		
Mass flow rate (lbm/hr)	30.8	
Power (Watts)	1046.0	
Heat Load (Watts)	334.4	
State Point	Temperature (° C)	Pressure (psia|kPa)
1	-3.6	10.4
2	98.6	158.5
3	23.5	158.5
4	4.3	158.5
5	4.1	158.5
6	10.0	158.5
7	-23.4	158.5
8	-51.3	10.4
9	9.3	10.4
10	-78.7	10.4
11	-75.2	10.4
12	-69.5	10.4
13	-64.7	10.4
14	-59.3	10.4
15	-46.0	10.4
16	-15.5	10.4
17	2.8	N/A
18	1.9	N/A

Test five is extended to analyze the mixed refrigerant system with the new mixture ratio at a compression ratio of 12:1, similar to test 2. Test six is performed with a suction pressure of 11 psia and a compression ratio of 12:1. System pressures for test six are presented in Figure C.11 and the temperatures recorded in the evaporator are presented in Figure C.12. Recorded measurements for test five are found in Table C.6.

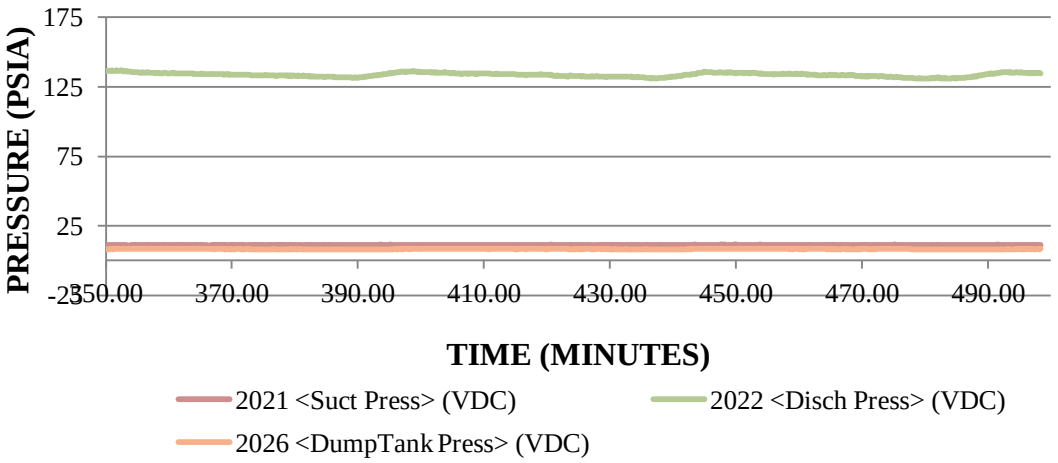

Figure C.11: Test 6 system pressures for 40% R23 and 60% R134a mixture ratio.

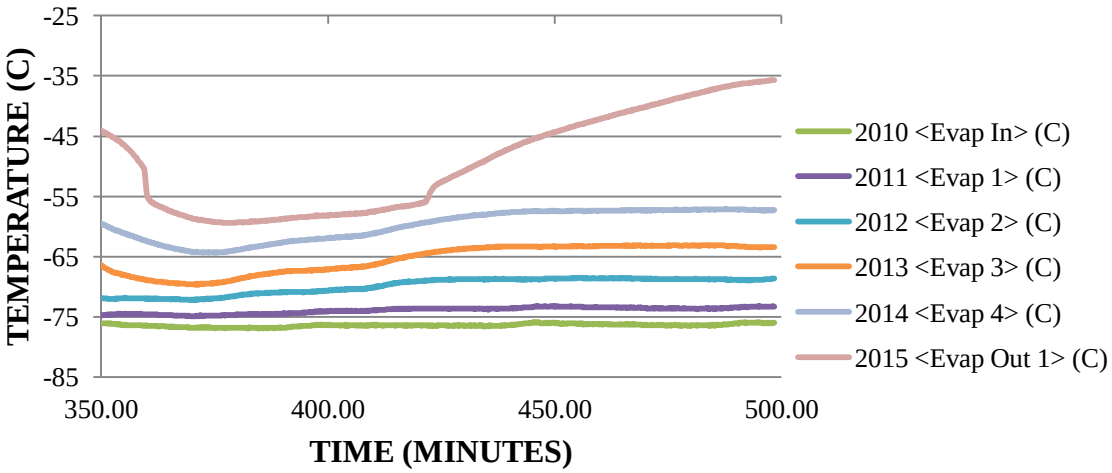

Figure C.12: Test 6 temperatures recorded in the evaporator.

Table C.6: Test 6 results with mixture ratio of 40% R23 and 60% R134a.		
Mass flow rate (lbm/hr)	45.4	
Power (Watts)	1214.1	
Heat Load (Watts)	516.2	
State Point	Temperature (°C)	Pressure (psia)
1	-5.0	11.2
2	105.2	134.6
3	22.3	134.6
4	2.6	134.6
5	1.6	134.6
6	6.4	134.6
7	-32.2	134.6
8	-47.6	11.26
9	5.0	11.2
10	-75.9	11.2
11	-73.2	11.2
12	-68.6	11.2
13	-63.3	11.2
14	-57.2	11.2
15	-35.6	11.2
16	-12.7	11.2
17	1.0	N/A
18	0.5	N/A

Table C.7: Experimental state points for Test 1 at suction pressure of 11 psia and compression ratio of 15:1 (66.6% R134a|33.4% R23)

States	P (psia)	T (°F)	H (Btu/lbm)	s (Btu/lbm-R)
1	11.0	-5.8	100.7	0.2553
2	163.8	212.4	140.3	0.2681
3	163.8	71.1	90.1	0.1808
4	163.8	51.6	29.7	0.0631
5	163.8	49.6	98.8	0.2061
6	163.8	55.1	103.1	0.2144
7	163.8	-3.92	11.5	0.0258
8	11.0	-50.5	29.7	0.0773
9	11.0	53.7	112.5	0.2720
10	11.0	-101.8	11.5	0.0386
15	11.0	-71.6	66.5	0.1874
16	11.0	-44.2	73.6	0.1907

Table C.8: Experimental state points for Test 2 at suction pressure of 11 psia and compression ratio of 12:1 (66.6% R134a|33.4% R23).

States	P (psia)	T (°F)	H (Btu/lbm)	s (Btu/lbm-R)
1	11.5	18.9	105.1	0.2638
2	131.6	218.4	142.5	0.2760
3	131.6	70.7	108.9	0.2199
4	131.6	45.1	27.1	0.0582
5	131.6	43.9	100.4	0.2217
6	131.6	50.3	103.8	0.2185
7	131.6	-23.1	5.3	0.0120
8	11.5	-46.2	27.1	0.0690
9	11.5	46.9	111.5	0.2663
10	11.5	-98.9	5.3	0.02017
15	11.5	-60.2	78.9	0.2153
16	11.5	5.30	102.7	0.2586

Table C.9: Experimental results for Test 3 at suction pressure of 14 psia and compression ratio of 15:1 (66.6% R134a|33.4% R23).

States	P (psia)	T (°F)	H (Btu/lbm)	s (Btu/lbm-R)
1	14.0	47.8	110.3	0.2701
2	218.7	232.5	143.8	0.2672
3	218.7	72.4	60.0	0.1209
4	218.7	73.0	36.3	0.0756
5	218.7	73.6	104.5	0.2098
6	218.7	73.0	104.5	0.2095
7	218.7	23.1	20.4	0.0445
8	14.0	-37.3	36.3	0.0916
9	14.0	73.0	116.1	0.2738
10	14.0	-80.7	20.4	0.0604
15	14.0	-12.1	98.2	0.2580
16	14.0	36.9	108.3	0.2660

Table C.10: Experimental results for Test 4 at suction pressure of 14 psia and compression ratio of 12:1 (66.6% R134a|33.4% R23).

States	P (psia)	T (°F)	H (Btu/lbm)	s (Btu/lbm-R)
1	14.2	43.4	109.5	0.2681
2	172.2	231.1	144.5	0.2732
3	172.2	75.4	92.2	0.7831
4	172.2	72.9	36.2	0.0755
5	172.2	61.2	80.6	0.1644
6	172.2	63.3	84.7	0.1722
7	172.2	2.30	13.3	0.0296
8	14.2	-33.3	36.2	0.0875
9	14.2	61.3	114.5	0.2652
10	14.2	-84.9	13.3	0.1049
15	14.2	-9.54	99.4	0.2520
16	14.2	36.5	108.2	0.2655

Table C.11: Experimental results for Test 5 at suction pressure of 11 psia and compression ratio of 15:1 (60% R134a|40% R23).

States	P (psia)	T (° F)	H (Btu/lbm)	s (Btu/lbm-R)
1	10.4	25.5	105.9	0.2722
2	158.5	209.5	139.2	0.2694
3	158.5	74.5	108.1	0.2176
4	158.5	39.7	25.3	0.0545
5	158.5	39.4	99.0	0.2011
6	158.5	50.1	102.1	0.2155
7	158.5	-10.1	9.6	0.0216
8	10.4	-60.4	25.3	0.0686
9	10.4	48.9	111.2	0.2741
10	10.4	-109.8	9.6	0.0346
15	10.4	-50.9	91.4	0.2574
16	10.4	3.95	102.1	0.2640

Table C.12: Experimental results for Test 6 at suction pressure of 11 psia and compression ratio of 12:1 (60% R134a|40% R23).

States	P (psia)	T (° F)	H (Btu/lbm)	s (Btu/lbm-R)
1	11.2	22.9	105.4	0.2693
2	134.6	221.5	142.5	0.2779
3	134.6	72.2	108.9	0.2223
4	134.6	36.8	24.4	0.0528
5	134.6	35.0	97.5	0.2087
6	134.6	43.6	102.0	0.2178
7	134.6	-26.1	4.4	0.0099
8	11.2	-53.8	24.4	0.06356
9	11.2	41.1	110.0	0.2669
10	11.2	-104.8	4.4	0.0187
15	11.2	-32.2	94.6	0.2602
16	11.2	8.9	102.9	0.2640